AGAVE

Project number: COOP-CT-2005-017668

Project acronym: AGAVE

Project title: AGV Navigation system based on a flexible and innovative UWB positioning

Instrument: Cooperative Research

Publishable Final Activity Report

Period covered: from M1	to M27	Date of preparation:	1/04/2008
Start date of the project	01/10/2005	Duration:	27 months
Project coordinator name	Paolo De Stefanis		
Project coordinator organisation name	LABOR Srl	Revision	0

TABLE OF CONTENTS

SECTION 1 Project execution 3

1.1 Project objectives 3

1.2 Contractors list 9

1.3 Work performed 10

1.4 Final results 12

1.4.1 AGAVE specifications and design 12

1.4.2 Positioning software development 19

1.4.3 Data fusion algorithms 29

1.4.4 System prototyping and installation 54

SECTION 2 Dissemination and use 66

2.1 Description of exploitable results 66

2.1.1 All in one integrated system for vehicle guidance 66

2.1.2 Localization system and algorithms 71

SECTION 1 Project execution

1.1 Project objectives

The overall objective of the AGAVE project is the development of an advanced guidance system for Automatic Guided Vehicles, focusing on the development of a next generation positioning system, allowing both indoor and outdoor transportation with unparalleled flexibility.

The target of the project is to make available a totally innovative free-range navigation system, allowing integrated operation and instantaneous transition in indoor and outdoor environments, even over very large areas.

AGAVE will be far beyond existing solutions, providing easy adaptation to production environment changes, improving overall quality, reducing total lead-time.

The core of the innovation will be the AGAVE positioning system, implemented thanks to the application of advanced sensor fusion techniques, for the concurrent and synergetic exploitation of three complementary positioning approaches (a scheme of principle is reported in Fig.1).:

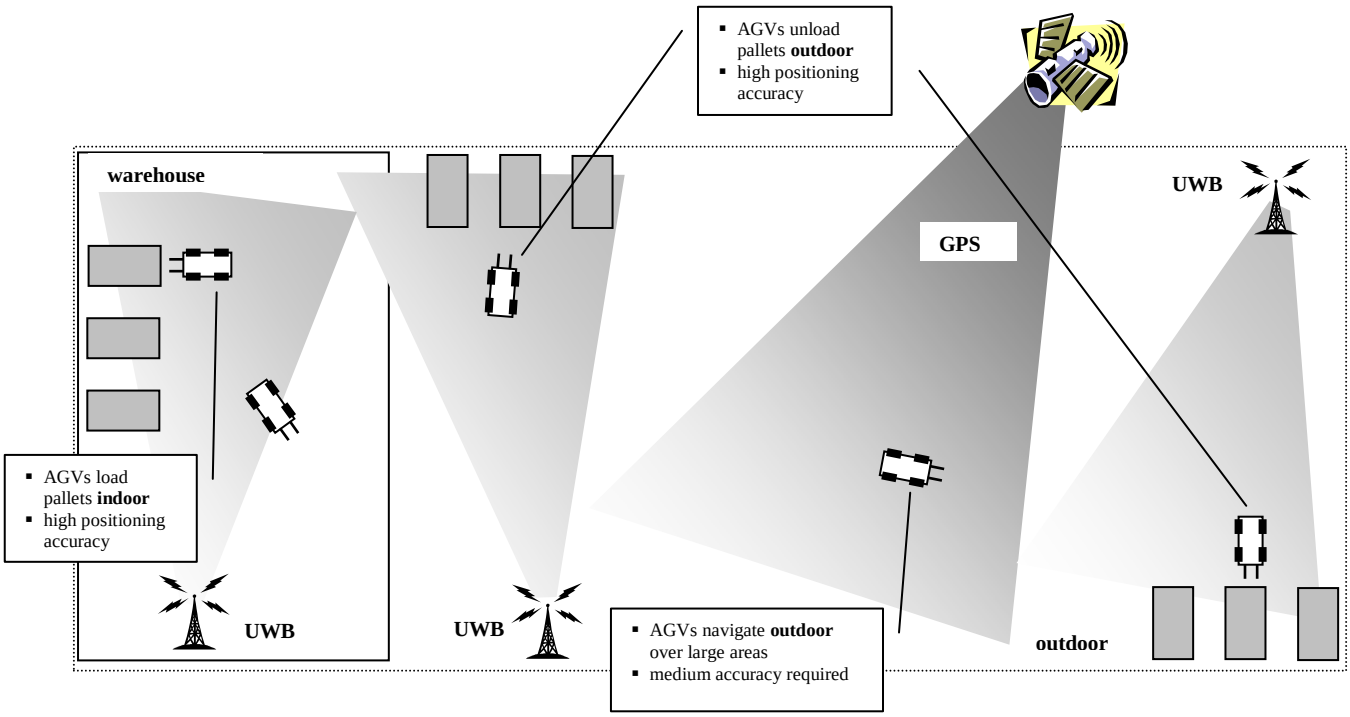

Fig.1 – Scheme of principle of AGAVE system

1. Ultra Wide Band (UWB) for indoor and outdoor short/medium range navigation, with high positioning accuracy (loading and unloading from operating machines)

2. Differential GPS for outdoor, long/very long range navigation with medium positioning accuracy
3. Dead reckoning (odometer) for continuous instantaneous information from wheel encoders and, possibly, gyroscope

An automatic guided vehicle (AGV), also known as a self guided vehicle, is an unmanned, computer-controlled mobile transport unit that is powered by a battery or an electric motor. AGVs are programmed to drive to specific points and perform designated functions.

They are becoming increasingly popular worldwide in applications that call for repetitive actions over a distance. Common procedures include load transferring, pallet loading/unloading and tugging/towing. Different models, which include forked, tug/tow, small chassis and large chassis/unit load, have various load capacities and design characteristics. They come in varying sizes and shapes, according to their specific uses and load requirements.

AGVs have onboard microprocessors and usually a supervisory control system that helps with various tasks, such as tracking and tracing modules and generating and/or distributing transport orders.

They are able to navigate a guide path network that is flexible and easy to program. Various navigation methods used on AGVs include laser, camera, optical, inertial and wire guided systems.

The true innovation of this project is represented by the UWB positioning technique, thoroughly new and never applied in such a context that allows overcoming the drawbacks of the above noted driving systems.

For instance it can be now possible to drive a vehicle without the need of Line Of Sight conditions, as in the case of laser guidance systems, thus allowing a smaller amount of beacons; moreover laser can not be used in harsh environments, such as refrigerators or very hot places. AGAVE system consists of the computer, software and technology that are the “brains” behind the AGV. A block diagram of the operating principles of the system is sketched in Figure 2.

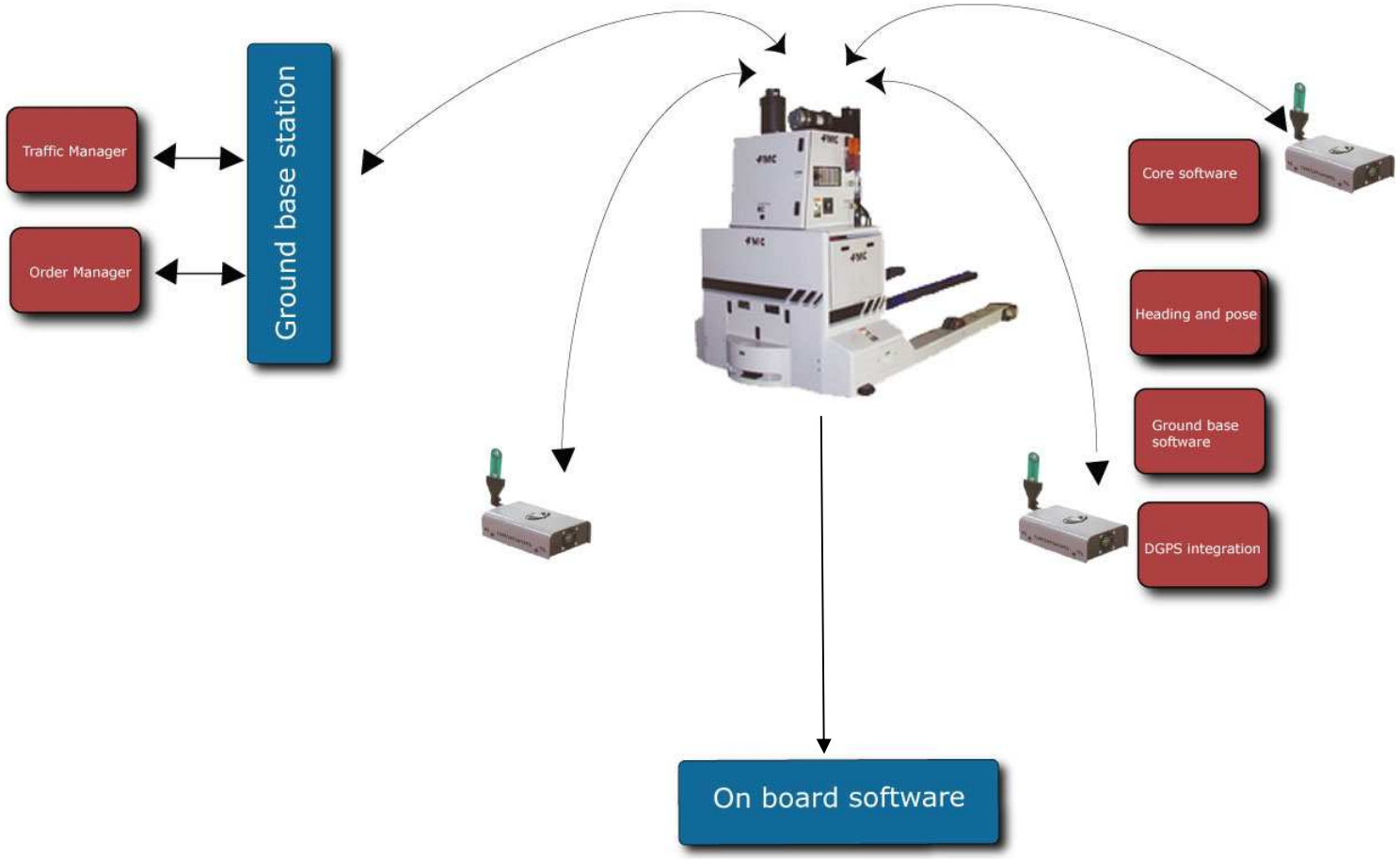

Fig.2 – Block diagram of AGAVE system

AGAVE guidance system will be composed of the following main elements:

1. **Positioning module**, that exploits UWB technology to obtain the two dimensional position of the vehicle with respect to the floor map of the plant, providing the navigation module with the x,y coordinates with an accuracy of (in the worst case) $\pm$ 1 cm, suitable both for the navigation and the docking phases.

2. **Navigation module** providing AGV guidance and real time communication with the fixed host station for fleet management and route optimisation, comprising the data fusion techniques based on Monte Carlo particle filters for integrating the inputs from DGPS, odometry, UWB and gyroscope, providing a reliable position and bearing estimation to the driving actuators (steering and motor controllers).

3. **Communication module** providing on line wireless data exchange between the fleet and the central supervision unit; this will be achieved by means of radio communication.

4. **Collision avoidance** by means of proximity sensors to avoid the collision with obstacles. These sensors are security devices, such as electronic bumpers, that check the area surrounding the vehicles in order to force, if necessary, the vehicle to slow down or stop.

5. **Central supervision** unit for advanced fleet management, communicating wireless in real time with all the vehicles and performing continuously route optimisation; the development of a new, specialised and flexible central supervision unit is a key objective for the full exploitation of the AGAVE concept; AGAVE is expected to provide a class of performance which was unachievable so far, which could make it possible to exploit it for much wider exploitation than the AGV only; high positioning accuracy can be provided through small and (especially in the future) cheap mobile units, and these can be used, for instance, to localise items, or people, in a given volume, in a number much higher that a fleet of industrial vehicle. The most important innovation in this field will be the implementation of the algorithm for optimal route selection and for deadlock prevention, that will lead to an increase of the performances of the plant in terms of execution time of the processes.

The odometer, the navigation module and collision avoidance are already available in NuovaFima's range of vehicles based on laser positioning and require further integration with the performance of the novel positioning system; further work is necessary to define proper integration by sensor fusion; the fixed host station needs to be substantially enhanced in order to match the potentialities of the other components and incorporate all consequent improvements.

The following are typical values for precision and repeatability errors in industrial mobile robotics applications, and will be the reference values for the AGAVE guidance system:

The target accuracy for position and heading errors (e, δ) will be as follows:

AGAVE objectives					
Accuracy		UWB		UWB + GPS	
		Position error (e)	Heading error (δ)	Position error (e)	Heading error (δ)
	v=0 m/s	± 10 mm	± 0,1°	≤ ± 8 cm	≤ 0,2°
	v=1m/s	± 20 mm	± 0,2°	≤ ± 15 cm	≤ 0,3°
Maximum Range (m)		200		5.000	
POS + TLC System cost (€)	< 5.000				
Time to market (months after the end of the project)	12-15				

The main technical advantages of the AGAVE system are:

- to operate in a very wide warehouse, indoor with a medium route 150 - 200 m
- to realise a very flexible system, easily to be adapted to an outdoor application with medium route envisaged 4 - 5 Km
- to be compatible with all possible configurations of the AGV, even platform carriers, which is currently impossible with laser based positioning systems
- to be compatible with all possible layouts of the warehouse, with narrow corridors or with the occupation of the overhead volume now kept free to ensure line of sight conditions for laser systems.
- To be easily manageable and configurable by means of an advanced user's interface
- to well automate the logistic phase of goods transportation, ensuring a smooth functioning of the several pick and drop phases requested
- to reduce the total lead-time of the entire industrial process

Further targets are identified as follows:

- **AGAVE flexibility**

  Flexibility is intended as the capability to reconfigure easily the paths of the AGV after a change of the warehouse layout, i.e. the addition of a palletiser or of a unloading station; AGAVE will be able to perform this operation via SW, without the need to reconfigure the accessories in the require area.

- **AGAVE standardisation**

  The current adopted AGV system are special purpose handling systems, that means designed and developed for the specific "autonomous" applications; this limit is profitably overcome by the AGAVE system thanks to its high expected modularity; in fact the AGAVE building blocks, such as control system, electrical motors, drives etc. are standardised to a high degree which keeps the costs down on a competitive level.

- **AGAVE reliability**

  Great reliability of the whole system in executing the operational tasks as requested by the working program; the AGAVE system is able to realise a self-optimisation during its functioning. Moreover the system is able to guarantee high precision standard in positioning and thanks to the security devices adopted any kind of accidents during the working program execution will be completely avoided.

- **AGAVE cost effectiveness**

  Installation costs are the crucial factor to be targeted; laser systems require the installation on peripheral walls of a highly redundant number of reflectors, each of them placed with mm precision with a theodolite; buried inductive transponders can be placed with a drill hole on the floor, but their precision is one order of magnitude lower (less than 10 cm, considering a system with a transponder each 10 m). AGAVE can provide laser like accuracy at installation costs which are higher than those of inductive transponders, but certainly lower than those of laser systems.

1.2 Contractors list

Table 1– List of participants

Partit. role	Partic. type	Partic. No.	Participant name	Participant short name	Country	Date enter project	Date exit project
CO	RTD	1	LABOR S.r.l.	LABOR	I	Month1	Month 27
CR	SMEP	2	Nuova Fima SpA	NuovaFima	I	Month 1	Month 27
CR	SMEP	3	Proceram GmbH	Proceram	D	Month 1	Month 27
CR	SMEP	4	Dirk Shumann Formen und Machinenbau GmbH	Machinenbau	D	Month 1	Month 27
CR	SMEP	5	Cosmotek S.r.l.	Cosmotek	I	Month 1	Month 27
CR	SMEP	6	Mesurex S.L.	Mesurex	E	Month 1	Month 27
CR	RTD	7	University of Udine	UniUD	I	Month1	Month 27
CR	RTD	8	Instituto Agilus de inovação em Tecnologia de Informação Lda.	IAITI	P	Month1	Month 27
CR	RTD	9	University of Malaga	UMA	E	Month1	Month 27

1.3 Work performed

The work performed in the project was divided in the following Work-packages:

1) WP1 Preliminary study of the navigation system

- A common reference framework to codify target characteristics and performance from the end-users' side was crated, to constitute a reference framework for the entire project. The main requirements defined were:
    - linear and angular positioning accuracy for indoor and outdoor navigation
    - linear and angular positioning accuracy for precision loading/unloading
    - AGV commercial speed
    - acceptable variation of positioning accuracy depending on speed
    - DGPS positioning
    - data exchange protocols and standards in use
    - draft configuration of the AGV navigation system
    - costs range
    - all other specifications which constitute boundary conditions for the AGAVE system

- Definition of the typical requirements for the HW which is expected to be used in industrial AGVs and related fleet management systems; production of a list of optimised expected performance.

2) WP2 Navigation and fleet management

- Implementation of the backbone fleet management system for the exploitation of the advanced capabilities of the AGAVE navigation system, able to cope not only with standard AGV navigation inside an industrial environments, but also with a larger number of applications, which may differ as far as the following variables are concerned:
    - Number of mobile units to be monitored
    - Accuracy of measurements
    - Navigation range
    - Information exchanged with mobile units
    - Security issues
- Two modules were made available:

- Mobile navigation module, installed on every AGV, or moving item, implementing dead reckoning, data fusion and vehicle guidance
- Ground based host navigation module, implementing fleet management, route optimisation

3) WP3 Ultra Wide Band lab testing

- Measurements of native positioning capabilities of UWB Pulse-on chips were performed
- Data transfer performance of Pulse-on chips in the target environment were assessed
- Risk assessment on UWB technology
- Measurements in anechoic chamber

4) WP4 Electronic design

- Design of a stand-alone system specialised in high precision measurement of position and bearing of a mobile unit respect to a network of fixed emitters through UWB signalling, including data transfer capabilities based on the same technology
- Design of the system for calculating of AGV bearing respect to a fixed axis
- Firmwareupgrade, which will allow correct operation of the system and adequate real time management of clock synchronisation for the various input signals.

5) WP5 Positioning and data fusion

- Selection of the computational methods for positioning
- Implementation of the algorithms to perform signal filtering and data fusion to produce best accuracy.

6) WP6 Alpha prototype (POS and TLC) development and testing

- Manufacturing of the Alpha prototype
- Laboratory and field alpha testing

7) WP7 Beta prototype (POS and TLC) development and testing

- Manufacturing of the Beta prototype
- Laboratory and field beta testing

8) WP8 Exploitation and dissemination of results

- Market study
- Exploitation strategy for AGAVE

- Dissemination of AGAVE

1.4 Final results

The main results achieved by AGAVE project are described in the following sections:

1.4.1 AGAVE specifications and design

Nuova Fima has been working in the automatic machine sector for ceramic industry for over twenty years. By exploiting its experience and skills and by availing of a by now consolidated structure, the company can produce based on Laser Guided Vehicles (LGV) used to handle various types of loads (pallets, boxes, rolls of paper or tissue).

The Nuovafima AGV was developed exclusively for the automated material handling process of tile manufacturing but lends itself seamlessly to a broad range of material handling applications. The AGV features SICK navigation and bumper protection technology and a PC based on-board vehicle controller. The superior control system allows for instantaneous revisions to both paths and destinations with a simple “click and drag” feature. This feature will be demonstrated as show attendees are given the opportunity for a “hands-on” programming session.

Products acquire an advanced control technology where you can literally sit down and change the system guide-path and destination in just a few seconds.

Nuovafima’s vehicles have to service a diverse group of industries, including aerospace, government, manufacturing, newspaper and printing, warehousing and automotive.

AGVs help automate material handling and they actually improve response time for material movement; they are suitable for short and long distance moves with the ability to fit into tight areas and to share aisles with operators and manual fork lift traffic.

1.4.1.1 Linear and angular accuracy for navigation

In the table below the accuracy provided by laser device currently deployed by Nuovafima’s vehicles is depicted:

INDOOR NAVIGATION

Speed	Linear accuracy Position error (e)	Angular accuracy Heading error (δ)
Docking Speed: v=0 m/s	± 4 mm	± 0,1°

Navigation Speed v=1.5 m/s	± 6 mm	± 0,2°

However the accuracy needed for safely and reliably driving an AGV is more relaxed, leading to the following requirements:

INDOOR NAVIGATION

Speed	Linear accuracy Position error (e)	Angular accuracy Heading error (δ)
Docking Speed: v=0 m/s	± 15 mm	± 0,2°
Navigation Speed v=1.5 m/s	± 50 mm	± 0,3°

These figures are in accordance with the first field tests results with UWB technology.

For what concerns outdoor navigation, these are the required figures:

OUTDOOR NAVIGATION

Speed	Linear accuracy Position error (e)	Angular accuracy Heading error (δ)
Docking Speed: v=0 m/s	± 15 mm	± 0,2°
Navigation Speed v=1.5 m/s	± 100 mm	± 0,3°

These figures can be achieved by means of the synergistic action of UWB and DGPS.

1.4.1.2 AGV specifications

AGV may be described as:

Towing AGVs:

- Steer Drive vehicle
- Designed to Deliver a Variety of Containers

- Single or Multiple Container Capability
- Load Capacities up to 1,500 Lbs.
- Equipped with Laser Bumper System
- All the models can tow single or multiple trailers and be configured for manual or automatic loading.
- Their benefit is in the ability to move considerably more loads with multiple trailers than a single fork truck.

Unit Load Carriers

- Dual Steer Drive vehicles
- Quad vehicles.

Unit load carriers feature rugged steel frame construction designed to function in industrial environments.

Unit Load Vehicles provide the backbone for high throughput operations. These highly manoeuvrable vehicles carry one or two loads at a time to facilitate the automatic transport and load transfer to and from conveyors, stands, production equipment, monorail, palletizing cells etc. In addition, unit load AGVs provide a perfect compliment for delivery to and from Automated Storage and Retrieval Systems (AS/RS).

Each model offers a unique combination of capacity, steering, load transfer and dimensional characteristics; a variable lift height system permit load pickup and drop-off interface with floor, stands or rack elevations.

The configurability of the lifting let the vehicle transport different kind of loads as racks, pallets, rolls and multiple loads.

The vehicle Features are:

- Fully symmetric, full speed, bi-directional

- Maximum layout flexibility
- Minimal floor space consumption
- Full keyboard/LCD panel interface with e-stop switch
- Local diagnostics and feedback
- Four point lifting
- Smooth non-binding lifting of off-center loads
- On-board microprocessor intelligence
- Complete navigation information resides in each vehicle
- Downloadable from system control center
- 48-volt batteries
- Quick charging for maximum vehicle utilization
- Minimized vehicle count 24/7 operation
- Side contact bumpers
- Side contact protection when turning
- Dual range laser obstacle detection at each end
- Fail safe non-contact protection
- Safe Class 1 lasers are used at floor level
- Four wheel stability
- Positive steering
- Load is equally distributed

Fork Vehicles

It is a Steer Drive vehicle:

The fork AGVs are used to move product from production lines to buffer and stretchwrap/shipping locations. Fork style vehicles provide the flexibility for picking and depositing loads to a variety of station types and elevations. Fork vehicles can interface with conveyors, load stands, racking and floor locations.

Many fork applications call for the pickup and transport of loads from a warehouse operation to shipping docks. “Deep Lane” staging of the loads by AGVs provides an efficient operation with minimal floor space. With this operation a loaded fork vehicle enters a floor lane and deposits the load by detecting the last pallet stored in that lane.

In other applications, fork vehicles provide inventory management by storing and retrieving loads within a rack structure. With lift capability to 20 feet, fork vehicles provide an ideal solution for working process buffers or servicing all aspects of a production facility or warehouse.

Besides timely and automated transportation, fork vehicles can incorporate a bar code or RFID reader that provides product identification and real time load tracking. These added benefits are key ingredients for a fully integrated and automated material delivery system.

Operators at the production lines hand stack boxes on pallets at floor level.

When a pallet is ready for transport, the operator will press an AGV call button.

The call signal is received by the AGV Vehicle Manager’s PC.

It communicates the calling station location to the host computer system. The host computer identifies the product type and gives the vehicle manager a destination for the load. The vehicle manager selects the closest available AGV to execute the pickup and delivery task.

The vehicle receives its mission via Radio Frequency instruction from the Vehicle manager. Loads picked up in the production area can be transported to either the buffer storage area or directly to the stretch wrap drop-off station in the shipping department.

Loads that are taken to the buffer area will be picked up by AGV at a later time.

Often the buffer area is double ended. Incoming loads are brought to one end of the system, while outgoing loads are picked up at the other end of the system.

This is the most popular vehicle for pallets with the following characteristic:

Mechanical structure:

- The triangular structure is made up of a vertical driven wheel with fixed motor and steering fifth wheel with gear pair. Wound driving motor with emergency brake, pair of idle wheels and cover in vulkollan.
- Maximum capacity of the vehicle: up to 3 000 kg.
- Hydraulic lifting control unit
- Powered by 48 V lead accumulators.

- Battery replacement system via side extraction with the use of a trolley supplied with the vehicle.

Technical characteristics:

- Automatic laser guided transpallet vehicle with support wheels at the side of the pallet.
- Possibility of being manually guided by means of a push button control panel that can be installed.
- Capacity: 2200 kg at 600 mm of its centre of gravity
- Max. lifting capacity: 2200mm
- Width of forking bay: 1180 mm
- Forged forks type FEM 2 (length 1200mm)
- Pallet forking from the ground with minimum bay height of 75 mm.
- Speed: adjustable up to a maximum of 70 m /min

AGV commercial speed

Navigation speed : min 0.2 m/s , max 1.5 m/s

Docking speed: max 0.2 m/s

Safety devices

- The front and back parts of the vehicle can be equipped with class 3 electronic laser bumpers.
- Two safety areas indicated as slow-down and stopping areas. Once the vehicle is beyond the hazardous area, it accelerates again or starts again automatically depending on the bumper area involved.
- Side protection by means of mechanical bars and limit switches.
- The ends of the outriggers or some model of forks are mobile with micro stop switch.

Equipment supplied

- 48 V / 250 Ah battery
- 3 incremental encoders for controlling the driving, steering and lifting movements.
- Mechanical “pallet presence” feeler
- Mechanical “pallet overlapped” control device
- Hydraulic top clamp that blocks the load on the pallet with stroke of 380,..,1200 mm

Communication System

The communications system is a combination of wired and wireless LAN. An Ethernet LAN connects the system control center to stationary elements including operator input terminals, RF antennas, lights,

sensors and interfaces with fire doors, elevators, and cart washers. A dedicated RF communications system communicates with vehicles.

Battery Charger

The battery charger consists of a wall-mounted power supply panel connected to charge rails embedded in the floor. Charging is on an opportunity basis, per vehicle as directed by the system control center. A safe feedback communications link requires a vehicle to be positioned on the rails in order for power to be applied.

1.4.1.3 HW requirements

The general technical specifications typical for On-board microprocessor are:

- CPU Intel Celeron 850 MHz
- 512 Mb RAM
- 2 x 10/100 Ethernet
- 2 CANBus port
- PC/104 –Plus Form Factor
- Digital I/O module OPTO-22
- 92 channel DIO Module with fully buffered I/O lines
- PCMCIA/ISA interface
- 4 com port RS232/422

1.4.1.4 Ground base software

The Ground Base Station Traffic Manager software was developed by Nuovafima to control the AGVs (Automated Guided Vehicle) within a system. This software runs on all of the Microsoft Windows operating platforms including Windows 2000 and utilizes standard PC hardware.

The purpose of the Manager software is to manage vehicle orders, provide system traffic control, interface with plant equipment/software (may be inputs to the system initiating further system operation or may be outputs from the Ground base system resulting from system operation), store AGV system operating data in a relational database, and provide automatic backup of system and data. It also allows to direct the operation of the system by logging onto a network terminal or by using a PC equipped with an RF modem. System data can also be viewed real-time or historical data recalled.

The Manager software is a user-friendly, intuitive graphical tool and there is also the possibility to design every particular warehouse layout by means of the specific layout design software tool

The purpose of the layout design software is to graphically create and/or edit AGV (Automated Guided Vehicle) guide paths. It also allows the user to quickly and easily add, delete, or modify pickup and drop

points. A CAD version of customer plant layout is imported into layout design software to minimize redrawing time. Minimizing the number of beacons required is simple with the Target Optimization tool.

The main innovation individuated to be added to the traffic and order manager sections of the already developed ground base software are:

- Advanced traffic management algorithms and in particular the implementation of an optimal route selection algorithm
- A deadlock prevention approach

ODOMETRY

Odometry is the most widely used method for determining the momentary position of a mobile robot. In most practical applications odometry provides easily accessible real-time positioning information in-between periodic absolute position measurements. The frequency at which the (usually costly and/or time-consuming) absolute measurements must be performed depends to a large degree on the accuracy of the odometry system.

The AGV will deploy two incremental encoders for steering and driving monitoring that will be inputs to the data fusion algorithms implemented in the Navigation software.

1.4.2 Positioning software development

Leading edge detection algorithm improvements

The ranging software computes the distance between two devices in two steps. First, a routine called "uwbTxtoRxDiff()" returns a raw ranging measurement; second, a leading edge detection algorithm corrects the raw data finding the first channel echo in the multipath environment.

Since the raw distance is computed by the FPGA, we can only try to improve the leading edge detection algorithm. This routine processes a buffer called *scan* which contains the same waveform saved by the scan-log command present in the Ranging Analysis Module; as far as we can understand, the vector *scan* is the sampled output of the receiver correlator. Thus, it corresponds to an estimate of the channel impulse response and so, the first peak of this response should correspond to the first channel echo.

Obviously, this channel estimation is affected by noise. So, to improve the detection of the first path, we may try to use averaging in the time domain. That is, we average the vector *scan* over time for successive measurements. Since the poor computation power of the microprocessor mounted on the PulsON 210 UWB kit, the method we propose is a simple first order recursive filter which purpose is to implement the weighted average between the new buffer and the priors. The expression of the IIR filter is:

$$\mathrm{avg_n}[i] = (1-\lambda)\,avg_{n-1}[i] + (\lambda)\,scan_n[i]$$

where $avg_n[i]$ is the i-th term of the weighted average at the n-th instant, $scan_n[i]$ is the i-th term of the correlation vector at the n-th instant and λ is the weighting factor. If the buffer *scan* represents the output of the correlator we can detect the leading edge looking for the maximum of the energy into a sliding window. The size of this window is determined by the channel duration. For indoor environments a typical value may be 10 ÷100*ns*.

CHAUVENET'S CRITERION

The ranging measurements obtained by the PulsON 210 UWB kit are affected by a certain number of outlier values. To try to eliminate these unwanted values the measurements can be filtered according to the Chauvenet's criterion which gives a simple test for deciding whether to reject the suspect data.

Suppose you have made *N* measurements:

$$x_1, x_2, \ldots, x_n$$

of a single quantity *x* , and if one of the values (call it x_{sus}) is suspiciously different from all the others.

First, compute the mean ($\bar{x}$) and standard deviation (σ_x) of all *N* measurements and then find the number of standard deviations by which x_{sus} differs from *x* :

$$t_{sus} = \frac{x_{sus} - \bar{x}}{\sigma_x}$$

If we assume the measurements were governed by a Gauss distribution whit mean *x* and standard deviation σ_x , we can calculate the probability of obtaining measurements that differ at least $t_{sus}\sigma_x$ from $\bar{x}$:

$$\mathrm{Prob}\left[\text{outside } t_{sus}\sigma_x\right] = 1 - \mathrm{Prob}\left[\text{inside } t_{sus}\sigma_x\right] = 1 - \int_{\bar{x}-t_{sus}\sigma_x}^{\bar{x}+t_{sus}\sigma_x} \frac{1}{\sqrt{2\pi}\sigma_x} e^{-\frac{1}{2}\left(\frac{a-\bar{x}}{\sigma_x}\right)^2} da$$

Now considering the variable substitution:

$$b = \frac{(a-\bar{x})}{\sigma_x}$$

from the formula above we obtain:

$$\mathrm{Prob}\left[\text{outside } t_{sus}\sigma_x\right] = 1 - \int_{-t_{sus}}^{+t_{sus}} \frac{1}{\sqrt{2\pi}} e^{-\frac{1}{2}b^2} db = 1 - \left[\Phi(t_{sus}) - Q(t_{sus})\right] = 1 - erf\left(\frac{t_{sus}}{\sqrt{2}}\right)$$

Given *N* measurements, for the property of the independent events, the number of measurements expected to deviate this much is:

$$n = N \times \text{Prob}\left[\text{outside } t_{SNS}\sigma_x\right] = N \times \left[1 - erf\left(\frac{t_{SNS}}{\sqrt{2}}\right)\right]$$

If $n < 0.5$ you can reject the value x_{sus} .

In others words, Chauvenet's criterion, as normally given, states that if the expected number of measurements at least as deviant as the suspect measurement is less than one-half, then the suspect measurement should be rejected. Obviously, the choice of one-half is arbitrary, but it is also reasonable and can be defended.

The following describes the algorithm used for calculating the position of the mobile vehicle, first describing the technical approach to the problem and then laying out the paths the led to the formulation of the final algorithm developed by Labor.

Classical ranging transactions (namely the Two Way Ranging -TWR- and the One Way Ranging -OWR- schemes), and the corresponding synchronization requirements, are highly dependant on the communication protocol and the network topology. The technique enabling to measure the signal round-trip Time-Of-Flight (TOF) between two asynchronous transceivers and that will be implemented in AGAVE consists in using a classical two-way remote synchronization technique. A pair of terminals are time-multiplexed with half-duplex packet exchanges. This procedure relies on a typical mechanism for fused location and communication: a requestor sends packets to a responder which replies after synchronizing with packets containing synchronous timing information. The reception of this response allows the requestor to determine the round-trip TOF information . This solution seems to be particularly adapted for distributed networks (a fortiori in the lack of coordination).

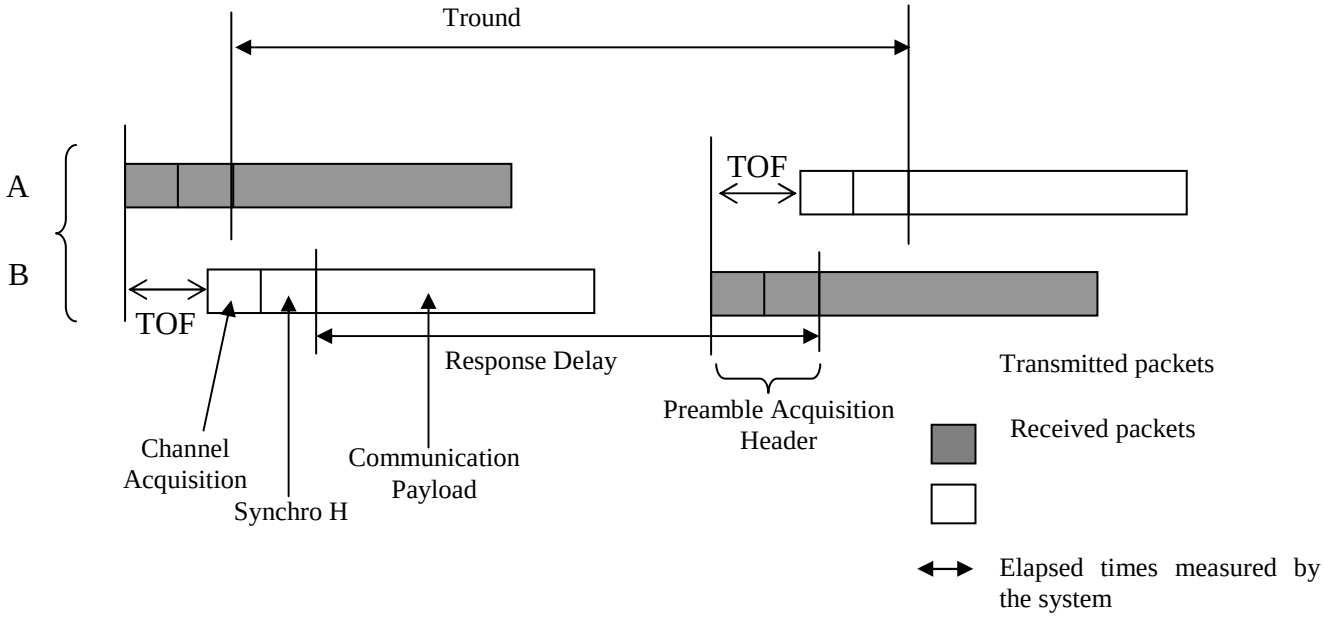

Figure 3: Two Way Ranging (TWR) transaction enabling to estimate the round-trip Time-OF-Flight between two asynchronous terminals (feeding TOA-based positioning algorithms)

For this kind of scenario, slot lengths and procedures fixed by a pre-existing communication standard represent drastic constraints for the maximum and minimum (blind distances) relative measurable distances, and the ranging accuracy. A straightforward approach uses a geometric interpretation to calculate the intersection of circles for TOA-based algorithms. Indeed, if three TOA are measured between a mobile terminal and three (or more) distinct anchors (note that anchors should be considered as nodes doted with a prior knowledge of their relative positions), the mobile position can be easily computed in the 2-D plane. These solutions (geometrical solutions or solutions based on optimization procedures) correspond to popular radiolocation methods, but it is not the purpose of the very document to focus on these positioning algorithms.

Ranging Errors from Relative Clock Drifts and Response Delays

When referring to Figure 3, one could easily obtain the following expressions:

$$2T_{OF} + \frac{T_1}{1+\Delta_{PNC}+\varepsilon} = \frac{T_1}{1+\Delta_{PNC}} + \frac{2\tilde{T}_{OF\,PNC}}{1+\Delta_{PNC}}$$

and

$$2T_{OF} + \frac{T_2}{1+\Delta_{PNC}} = \frac{T_2}{1+\Delta_{PNC}+\varepsilon} + \frac{2\tilde{T}_{OF\,DEV}}{1+\Delta_{PNC}+\varepsilon}$$

Where T_1, T_2 represent response delays, T_{OF} and $\tilde{T}_{OF}$ respectively the real and estimated TOFs, $(\Delta_{PNC}+\varepsilon)f_0$ and $\Delta_{PNC} f_0$ the frequency offsets of DEV's and PNC's clocks relative to an ideal frequency f_0.

In the proposed ranging procedure (under the assumption of a correct detection), it can be shown that:

$$\tilde{T}_{OF\,PNC} = (1+\Delta_{PNC})T_{OF} - \frac{\varepsilon T_1}{2(1+\Delta_{PNC}+\varepsilon)}$$

and that

$$\tilde{T}_{OF\,DEV} = (1+\Delta_{PNC}+\varepsilon)T_{OF} + \frac{\varepsilon T_2}{2(1+\Delta_{PNC})}$$

Single TOF Estimation

If ranging is based on a single estimation $\tilde{T}_{OF\,DEV}$ or $\tilde{T}_{OF\,PNC}$ (available with single TWR transactions), the error on the range estimate due to clock drifts and protocol response delays is on the order of:

$$E_{DEV} = \tilde{T}_{OF\,DEV} - T_{OF} = (\Delta_{PNC} + \varepsilon)T_{OF} + \frac{\varepsilon T_2}{2(1+\Delta_{PNC})}$$

and

$$E_{PNC} = \tilde{T}_{OF\,PNC} - T_{OF} = \Delta_{PNC} T_{OF} - \frac{\varepsilon T_1}{2(1+\Delta_{PNC}+\varepsilon)}$$

Depending on Δ_{PNC}, T_1, T_2 and ε, these errors can be significant. Now, considering a usual range lower than 15m, or equivalently that the maximum time of flight TOF is lower than 50ns, and that the absolute drift is on the order of 10^{-5}, it is clear that the first terms involved in the previous expressions are much lower than 50ps, and hence, can be neglected.

So, generally speaking and in first approximation, we can say that the error committed on the range estimate is:

$$E_{DEV} = +\frac{\varepsilon T_2}{2(1+\Delta_{PNC})}$$

and

$$E_{PNC} = -\frac{\varepsilon T_1}{2(1+\Delta_{PNC}+\varepsilon)}$$

At this point, several parameters should be discussed:

- The value of the pre-convinced reply delay T_2, depending on the PNC's ACK
- The value of ε, depending on a preliminary drift compensation, or initial drift conditions at the initiation of the PicoNet; in other words.

A preliminary drift correction obviously implies a preliminary drift estimation between the PNC and the DEV. In other words, before performing the whole ranging procedure, the DEV could wait for beacon synchronization over a sufficient number of Superframes. This will impact the initial value of the term ε.

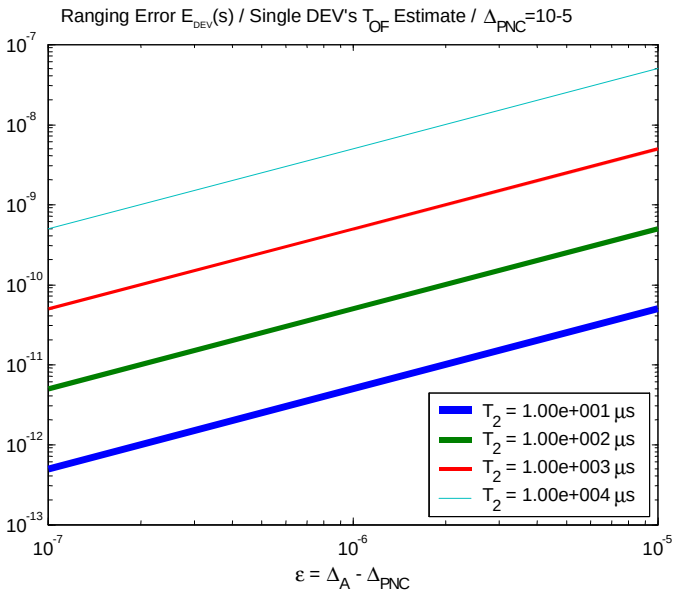

Figure 4 : Ranging Error with a Single DEV's T_{OF} Estimation (single TWR between the DEV and the PNC)

Actually, frequency offsets are random values. However, for the purpose of providing coarse but realistic specifications concerning ε and T_2, we can arbitrary set Δ_{PNC} to a pessimistic value of 10^{-5}. As shown on Figure 4, the ranging error for the single DEV's TOF estimation is maintained below 50ps for ε up to 10^{-5} if the ACK occurs within a duration less than 10µs. This corresponds to uncompensated drift situations when the value of ε is very large. Otherwise, when considering traditional values of ε = 10^{-6} (resp. 10^{-7}), the constraints on the ACK collapses down to 100µs (resp. 1000µs).

Two way ranging algorithm

The algorithm used to calculate the distance between the platforms is a simple two way time estimate process. T1 and T2 time intervals are evaluated by means of four timestamps: Tx1reg, Tx2reg, Rx1reg, Rx2reg. The first two timestamps are 25 bits long and have a resolution of 40 ns (they record the symbol time of frame transmission), whereas the last ones are 32 bits long and have a resolution of 1 ns (5 bits are used to represent the delay of the estimated first path, 1 bit indicates the path position in the neighbouring timeslot).

A complete description of the ranging algorithm follows:

- Start of ranging: device I sends a ranging frame to device II and a timestamp TX1reg is stored in a register;
- Device II receives the ranging frame, a timestamp RX2reg is stored;
- Device II answers the ranging frame, including the receiving timestamp RX2reg as well as the transmission timestamp TX2 in the data field of the frame;
- The shorter step leads to a more sharp synchronization, whereas the larger leads to faster but less precise results
- Device I receives the answer frame, estimates a receiving timestamp RX1reg and extracts the timestamps of device II to be stored in registers;
- After this cycle the four register values are passed to the application software, which calculates the distance with the formula in (3).

T1 = {Rx1reg(31:7) – Rx1reg(6) – Tx1reg(31:7)} * 40 ns + Rx1reg(5:0) * 1 ns. (1)

T2 = {Tx2reg(31:7) + Rx2reg(6) – Rx2reg(31:7)} * 40 ns – Rx2reg(5:0) * 1 ns. (2)

D = 0.5 * (T1 – T2 - offset) (3)

The first seven bits (0..6) of Tx1reg and Tx2reg are set to zero. The parameter 'offset' takes into account all the delays due frame processing. The ranging cycle is performed once per second and it lasts 1/2 ms.

Improving the performance of the algorithm

Figure 5 depicts a WAN consisting of reference tags with known position and mobile tags with unknown position. Assume that the WAN consists of $M=M_R+M_M$ tags, from which M_R tags indexed by i=1,2, ... , M_R are reference tags and M_M tags indexed by i= M_R +1, ..., M are mobile tags. The task of the WAN is to find the position of all mobile tags using the distance d_{ij} between the i-th and thej-th tag, where $_{ij}$=1,2, ... ,M. Figure 2 shows how to obtain d_{ij} using a two-way ranging (TWR) scheme. The tag i transmits a pulse to tag j, which itself responds by sending a pulse back to tag i. The distance d_{ij} is then given by:

$$d_{i,j} = c \cdot (t_{P,i} - t_{R,j})/2, \qquad (1)$$

where c is the speed of light, $t_{p,i}$ is the processing time of the TWR measurement, and $t_{R,J}$ is the reply time of tag j until it answers tag i with a pulse. To determine the processing and reply times in the TWR experiment, the periods P_i and P, of the clocks in the i-th and the j-th tag, respectively, is required, since only clock counters are available. We have $t_{P,i}=P_i n_{P,i}$ and $t_{R,i}=P_j n_{Rj,}$ where $n_{P,i}$ and n_{Rj} are the difference of the clock counter values at pulse transmission and arrival in the i-th and the j-th tag, respectively.

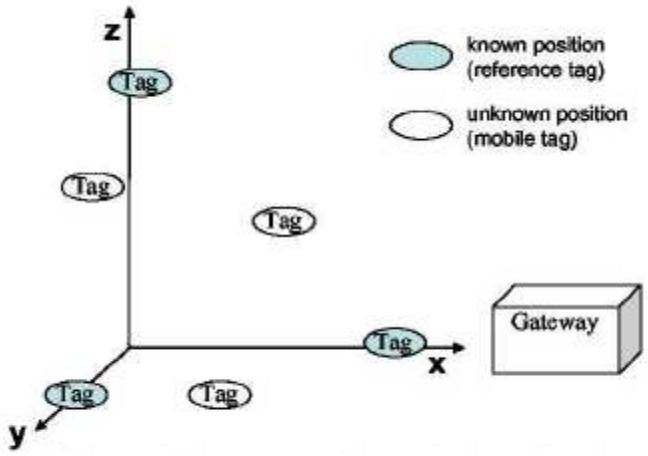

Figure 5: Wireless ad-hoc network consisting of reference tags with known position and mobile tags with unknown position

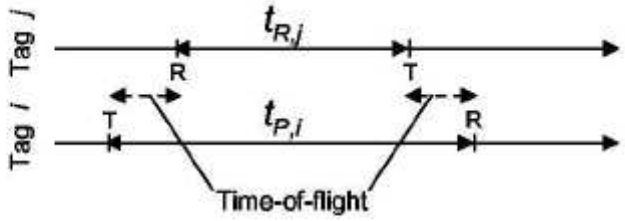

Figure 6: Pulse transmission schedule to calculate the time-of flight of a pulse transmitted between tag i and j

The tags assume that their clock periods are equal to the nominal value P, i.e., the tag calculates the following distance estimate:

$$\hat{d}_{i,j} = c \cdot P \cdot (n_{P,i} - n_{R,j})/2.$$

A relative bias Pi=(P_i-P)/P between the true clock periods P_i and P causes the following distance measurement error:

$$\Delta d_{i,j} = \hat{d}_{i,j} - d_{i,j} = c \cdot P \cdot (p_j n_{R,j} - p_i n_{P,i})/2.$$

Given the worst-case bias $p_{MAX}=\max |p_i|$ the maximum reply time $t_{R,MAX}=\max_j |t_{R,j}|$, and the longest time-of-flight $t_{F,MAX}$,the worst case distance error is

$$\max(\Delta d_{i,j}) = c \cdot p_{MAX} \cdot (t_{R,MAX} + t_{F,MAX}). \qquad (2)$$

The effect of the clock bias P_{MAX} on the distance measurement error depending on the reply time in the TWR experiment and the time of- flight is shown in Figure 6. Obviously, a larger clock bias can be traded for with a smaller reply time as long as the reply time is larger than the time of- flight. For our WAN application we are interested in a "raw" distance measurement precision below 5 cm. As shown in Figure 7, this is possible in a working range of 50m using clocks with a bias of 1000ppm (reply time is below l00ns) or 100ppm. Such clock biases are easily attainable with standard crystal clocks in the tags.

In the "reference-only" positioning mode, TWR is performed between reference and mobile tags, only, where always a reference tag initiates the TWR. Thus, the distances d_{ij} are calculated for i=l,..,M_R and j=MR+1,...,M, only, which gives a total of $M_M M_R$ measurements. In the "multi-hop" positioning mode, any pair of tags performs a TWR measurement. If this is done in one direction, only, i.e., the tag i initiates a TWR measurement to tag j, but not vice-versa, the total number of TWR measurements equals (M-1)xM/2. If two TWR measurements are carried out between a pair of tags, the measurement number is (M-1)xM.

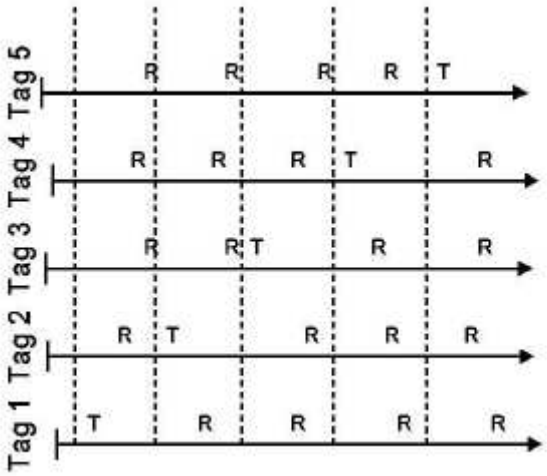

Figure 7: Pulse transmission schedule to perform TWR measurements between pairs of tags with high update rate

It has been shown in several measurement campaigns and articles that a sub-millimeter accuracy of measuring the distance between objects is possible based on ToA measurements of UWB RF pulses. We plan to utilize such pulses for finding the distances in between the tags of the WAN. In indoor

environments, however, the measured distances are erroneous according to the probability density function (PDF) given below,

$$p(\hat{d}) = \begin{cases} \exp(-(\hat{d}-d)^2/(2\sigma^2))/\sqrt{2\pi\sigma^2}, & \text{if LOS component is found} \\ \exp(-\hat{d}/D_M)/D_M, & \text{if LOS component is missed} \end{cases}$$

where d is the true and $\hat{d}$ is the measured tag distance. This PDF can be verified using real measurements or using simulations with standard indoor RF channel models. It turns out that the distance measurement suffers from zero-mean Gaussian-distributed error with standard deviation a if the tag receiver is able to find the LOS component of the RF signal traveling in between the tags. The parameter σ is the mm range using ToA measurements of ultra-wide band RF pulses, which is by far enough for the accuracy desired in our WAN (less than 5cm). If the LOS component cannot be found, e.g., because wall reflections yield multi-path components of stronger power, the distance measurement suffers from an exponentially distributed error with mean D_M. This parameter is in the m range, i.e., if the LOS component is missed, the distance measurement is useless. The problem is the rather high probability PM of missing the LOS component.

Calculating the positions x_i (X_i;,Y_i;,Z_i), i=M_R+ 1,...,M, of the M_M mobile tags from the measurements $d_{i,j}$, I,j=l, ...,M distributed with the PDF showed before is a real challenge. There exist algorithms for calculating the positions X_i by minimizing the square error between measured distances $d_{i,j}$ and the aligned distances after calculating X_i However, this approach assumes that the measurements are disturbed by a Gaussian-distribution error. However, this algorithm is difficult to implement. Furthermore, the parameters σ, P_M, and D_M are usually not available in a real application. A practical algorithm should be robust (no need of statistics) and simple to implement.

We propose the following approach: Assume that the i-th mobile tag has the measurements $d_{i,j}$ for j=l, ...,M_R from the M_R reference tags available, i.e., for simplicity we disregard the distance measurement in between the mobile nodes (no "multi-hop" positioning). Among the M_R measurements $d_{i,j}$ at least 4 are required to calculate the position x_i. Given the positions x_i,…., x_4 of 4 reference nodes, the mobile tag position x_i can be calculated directly from the measurements $\hat{d}_{i,1}, \cdots, \hat{d}_{i,4}$ as follows:

$$\mathbf{x}_i = \left[\begin{pmatrix} \mathbf{x}_2 - \mathbf{x}_1 \\ \mathbf{x}_3 - \mathbf{x}_1 \\ \mathbf{x}_4 - \mathbf{x}_1 \end{pmatrix}^{-1} \begin{pmatrix} (\mathbf{x}_2 - \mathbf{x}_1)(\mathbf{x}_2 - \mathbf{x}_1)^T - \hat{d}_{i,2}^2 + \hat{d}_{i,1}^2 \\ (\mathbf{x}_3 - \mathbf{x}_1)(\mathbf{x}_3 - \mathbf{x}_1)^T - \hat{d}_{i,3}^2 + \hat{d}_{i,1}^2 \\ (\mathbf{x}_4 - \mathbf{x}_1)(\mathbf{x}_4 - \mathbf{x}_1)^T - \hat{d}_{i,4}^2 + \hat{d}_{i,1}^2 \end{pmatrix}\right]^T + \mathbf{x}_1.$$

The Figure 8 shows the positioning performance in a WAN with MR=4 reference tags and MM=100 mobile tags using the positioning algorithm (4) and the distance measurement PDF (3) with σ=lmm, P_m=0.3 and D_m=2m to generate the distance measurements $\hat{d}_{i,j}$.

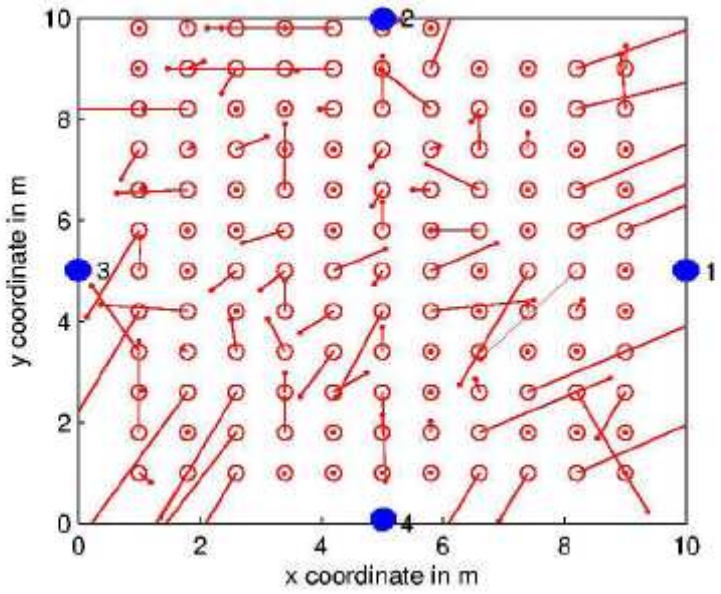

Figure 8: 3D positioning of MJ<FIOO mobile tags (circle: true position, dot: calculated position) in a WAN using distance measurements to MAr'I reference tags (thick circles)

The mobile tag position is very accurate if the tag receivers could find the LOS component in each of the 4 distance measurements. This happens with probability $P_{GOOD}=(l-P_M)^4$ which is only 0.24 for the chosen P_M. In the remaining cases, the mobile tag position is heavily disturbed, simply because the distance measurements have heavy errors. With M_R distance measurements available from M_R reference nodes, the probability $P_{BAD}=l-P_{GOOD}$ of not having 4 accurate measurements among them is given by

$$P_{BAD} = \sum_{k=0}^{3} \binom{M_R}{k} \cdot P_M^k \cdot (1-P_M)^{M_R-k}$$

It follows that the position X_i of a mobile tag can be calculated very accurately using the simple formula (4) from a set of 4 distance measurements where the LOS component of the UWB RF pulse was found. The question remains how to find such a set from the M_R available measurements $\hat{d}_{i,j}$, j=l, ... ,M_R. At this point the distance measurement error PDF in (3) with its heavy tail in case the LOS component has been missed comes as an advantage. It turns to be very simple to check whether a set of 4 distance measurements contains one belonging to a missed LOS component. The formula (4) was derived in [3] by calculating the point in which the 4 spheres with radius $\hat{d}_{i,j}$ spanned around the positions x_1, ..., x_4 of the reference nodes intersect. Errors in the distance measurements yield that the 4 spheres do not intersect in a single point anymore. We propose to check the error:

$$e_j = \left| \left\| \mathbf{x}_i - \mathbf{x}_j \right\|^2 - \hat{d}_{i,j}^2 \right| < threshold$$

between the squared measured distance $\hat{d}_{i,j}$ and that between the calculated mobile tag position x_i and the reference tag x_j to decide whether a set of 4 distance measurements contains all accurate

measurements. Using (4) to calculate x_i it can be shown that e_j is the same for any of the 4 reference tags indexed by j. Thus, among M_R distance measurements, we propose to search for quadruples of 4 measurements satisfying (5) after calculating X_i with this quadruple via (4). The necessary number of checks equals $M_R!/(4!(MR-4)!)$.

This number can be rather large, but the test equations (4) and (5) are very simple to implement, possibly in parallel.

1.4.3 Data fusion algorithms

1.4.3.1 Algorithm fundamentals

Mobile vehicle positioning is the problem of estimating the vehicle's pose (location, orientation) relative to its environment. Depending on the initial conditions of the vehicle, three categories of problems can be established. The former and simplest one is called in literature *position tracking*; in this situation, the starting pose of the vehicle is known, and the algorithms correct or compensate the errors derived from the odometry through sensory data. The second situation is the *global localization problem* or *wake-up vehicle's problem*, where the initial pose of the vehicle is unknown and has to be determined. The last problem is the *kidnapped vehicle problem*. In this case, a vehicle which knows its position is moved to a new localization without notification, so that it has the belief of being in some other place, with all the complications that this fact entails.

Most of the existing positioning algorithms only solve the position tracking problem since in that situation it is possible to make restrictive assumptions about the nature and shape of the errors and the vehicle uncertainty. There are classical approaches to the solution of the problem like lateration or triangulation but usually they do not deal appropriately with uncertainty, that is, they provide a given position estimate but no measure on the confidence on that position. Nowadays, some of the most efficient algorithms to deal with this problem are the probabilistic approaches based on Kalman filters, which provide elegant solutions for localization that are recognized to be optimal under uncertainty in the sensor measurements and actuators (motors) actions. However, these filters force both the noise and the uncertainty to be Gaussian distributed. These restrictions make them unable to cope with the global localization problem. Two families of methods have been proposed to deal with this issue: *multi-hypothesis Kalman filters* and *Markov Localization*. The former use mixtures of Gaussians with the purpose of representing each localization hypothesis with a different probabilistic distribution, but still have the restriction about the shape of the noise (in practice, this means that much of the information provided by the sensors is ignored, which is quite ineffective. The later uses piecewise constant functions over all the space of possible positions of the vehicle in order to represent complex multi-modal probabilistic distributions. Though many

improvements have been proposed, the main disadvantage of the Markov localization methods is that they are computationally expensive. Anyway, the probabilistic nature of all the mentioned methods is able to yield an optimal or near-optimal solution to vehicle positioning as well as a measure of the confidence that results. They are based on the estimation of a posterior probability distribution within the space of possible solutions (poses) under certain independence assumptions and a given knowledge on the initial localization of the vehicle. This approach is used in particular in Monte Carlo localization algorithms (MCL), a family of Markovian methods which present additional advantages over Kalman-based ones: MCL are capable to solve, in addition to the position tracking problem, both the global localization problem and the kidnapped vehicle problem. Furthermore, they can deal with any kind of noise distribution and non-linearities, and make unnecessary the extraction of features from the sensor data. This, along with the near-optimally of probabilistic methods, makes that, nowadays, Monte Carlo Localization seems to be one of the best solutions for localization problems.

MCL, also called Particle Filter, works by representing the posterior estimation of the possible vehicle poses by a set of weighted samples, or *particles*, which approximate the real objective probability distribution of the pose of the vehicle. Particle filters are state-of-the-art approaches also known in literature as Condensation Algorithms and have a number of advantages over the rest of methods for localization:

- They have the ability to work with almost arbitrary sensor characteristics, motion dynamics, and noise distributions.
- They do not need a restrictive assumption on the shape of the posterior density. It can be even multi-modal for representing several pose hypotheses simultaneously.
- Computational resources are well focused, since these methods sample proportionally to the posterior distribution.
- Since the number of particles can be modified, the algorithm can be adapted to the available computational resources, at the expense of the precision in positioning.
- Particle filters are easy to implement.
- They provide a suitable framework for the fusion of sensory information provided by different devices.

But basic Monte Carlo localization has also some disadvantages:

- Since the prediction is supported by particles, that is, by samples, a vehicle with a well-know position can loose its track because none of the generated samples is near the right pose.
- Derived from the latter, in the case of the kidnapped vehicle, it can happen that when the vehicle is moved to a new position no particle falls near this location.
- Finally, MCL requires the existence of different samples in order to approximate the vehicle pose. This means that, paradoxically, too accurate sensors cause the impoverishment of the sample space.

In spite of these limitations, there are practical approaches, as it will be seen through these pages, to overcome these problems and make possible the usage of Monte Carlo Localization in an efficient way.

Bayes Filtering

Bayes filters estimate a posterior probability density, called the *belief*, over a state space (possible poses of the vehicle) conditioned on the observation data. These filters are based in the *Markov assumption*, that is, the past and future data are (conditionally) independent; this means that the current state contains all the information needed to estimate the next state, which, as it will be seen later, allows us to implement recursive methods.

Most of the Markovian algorithms used today in localization are based on the Bayes Filter, where the posterior distribution representing the pose of the vehicle is estimated based entirely on collected sensor data, and denoted $Bel(x_t)$ (belief of being at *x* at a time *t*, being *x* the pose of the vehicle: typically, a set of two-dimensional Cartesian positions and an orientation). The description of Bayes filtering can be found in many bibliographic references, but no unified nomenclature has been proposed yet. Through this report we will follow the denominations used in, so the belief function will be represented as:

$$Bel(x_t) = p(x_t \mid d_{0..t}) \tag{2.1}$$

where $d_{0...t}$ are the data collected from sensors from time 0 up to time t. The data set can be separated into two subsets, depending on its nature: *odometry data* carry information about the vehicle motion, and we will denote them by *a,* for *action*; laser, GPS, UWB or other similar sensors provide *perceptual data*, which will be denoted by *o*, for *observation*. Thus,

$$Bel(x_t) = p(x_t \mid o_t, a_{t-1}, o_{t-1}, a_{t-2}, ..., o_0) \tag{2.2}$$

In order to derive a recursive update equation for $Bel(x_t)$, we apply Bayes rule to the former expression:

$$Bel(x_t) = \frac{p(o_t \mid x_t, a_{t-1}, ..., o_0)\, p(x_t \mid a_{t-1}, ..., o_0)}{p(o_t \mid a_{t-1}, ..., o_0)} \tag{2.3}$$

The expression $p(o_t \mid a_{t-1}, ..., o_0)$ is a constant, so (2.3) can be rewritten in this way:

$$Bel(x_t) = \eta\, p(o_t \mid x_t, a_{t-1}, ..., o_0)\, p(x_t \mid a_{t-1}, ..., o_0) \tag{2.4}$$

where the normalization constant is $\eta = p(o_t \mid a_{t-1}, ..., o_0)^{-1}$.

The Markov assumption implies that the future state is only dependent on the current one, so:

$$p(o_t \mid x_t, a_{t-1}, ..., o_0) = p(o_t \mid x_t) \tag{2.5}$$

The substitution of (2.5) into (2.4) yields:

$$Bel(x_t) = \eta\, p(o_t \mid x_t)\, p(x_t \mid a_{t-1}, ..., o_0) \tag{2.6}$$

Applying the total probability theorem, the expression for the belief, integrating over all states at time *t-1*, takes this form:

$$Bel(x_t) = \eta\, p(o_t \mid x_t) \int p(x_t \mid x_{t-1}, a_{t-1}, ..., o_0)\, p(x_{t-1} \mid a_{t-1}, ..., o_0) dx_{t-1} \tag{2.7}$$

The Markov assumption can be applied again, with the purpose of simplifying the first term in the integral:

$$p(x_t \mid x_{t-1}, a_{t-1}, o_{t-1}, a_{t-2}, ..., o_0) = p(x_t \mid x_{t-1}, a_{t-1}) \tag{2.8}$$

Now, if we consider the belief formula (2.2), we notice that it is present in the integral, thus a recursive equation can be finally obtained:

$$\boxed{Bel(x_t) = \eta\, p(o_t \mid x_t) \int p(x_t \mid x_{t-1}, a_{t-1}) Bel(x_{t-1}) dx_{t-1}} \tag{2.9}$$

This is the recursive update equation for Bayes filters. Now, jointly with an initial condition, it is possible to estimate the belief in a recursive way. There are two different starting situations: we can have knowledge about the initial state of the system, that will be the *initial belief*; or in cases like the global localization problem, this information will be unavailable, so the system will be typically initialized with a uniform distribution over the state space.

For the calculation of (2.9) two probability densities need to be known: $p(o_t \mid x_t)$ and $p(x_t \mid x_{t-1}, a_{t-1})$. The former is the *perceptual model* or *sensor model*, and depicts characteristics of the measurements provided by the sensors; the later is the *motion model* and reflects the behaviour of the odometry of the vehicle. Since both models are usually assumed as *stationary* (*time-invariant*), we can simplify the notation used, denoting:

$p(x' \mid x, a)$: motion model

$p(o \mid x)$: sensor model

In the following sections, we overview both models and the ways to obtain them.

Motion model

The model $p(x' \mid x, a)$ gives us the probability of finding the vehicle at a position *x'* after having performed the action *a* if its initial pose was *x*. This model is a probabilistic approximation of the vehicle kinematics and contains information about movement uncertainty.

As it has been mentioned before, for a vehicle moving in the plane, its pose typically comprises a set of two-dimensional Cartesian coordinates (*x*, *y*) and a heading direction (orientation or bearing, usually denoted as *phi*). The second variable, *a*, characterizes the change of pose and it can come from an odometric measure or a control command. The kinematical equation describes only the behaviour of the robot in a noiseless environment, that is, it represents the movement of an ideal noise-free vehicle, without considering the motion uncertainty. The modelling of the noise can be done in several ways: one of them is through a zero-centred additive Gaussian noise; other approximations consider the internal mechanisms that produce the noise and errors, and, for example, include the propagation of spatial uncertainty. This last method has been used in our experiments, and it will be explained in detail later on.

Sensor model

The sensor model $p(o \mid x)$ gives us the probability of having the observation *o* if the pose of the vehicle is *x*. This model is specific for each sensor and has to describe both the relation between the measurements and the position of the vehicle, and the uncertainty due to the noise in the measurement process.

If we consider only the sensors that will be used in the AGAVE project, the DGPS behaviour is well modelled, but we have not found in literature any reference describing how the UWB sensor works. For our first simulations we have used a Gaussian error model for the UWB system based in data collected from, though further modelling should be needed.

Monte Carlo Localization. Particle filters

Monte Carlo methods allow us to solve efficiently the Bayes Filter (2.9) by representing the belief function $Bel(x)$ by a set of weighted samples, or *particles*, distributed according to:

$$Bel(x) \approx \left\{ x^{(i)}, w^{(i)} \right\}_{i=1,\ldots,m} \qquad (3.1)$$

In this equation, the values $x^{(i)}$ are the particles (samples poses of the vehicle), that is, they are plausible poses following the established motion model. The *weights* $w^{(i)}$ are also called *importance factors* and represent the "goodness" of each particle for approaching the real belief function. This means that samples

with a higher weight will be nearer to $Bel(x)$ than other samples with smaller weights. In other words, the set of samples represent a discrete approximation of the continuous belief function.

In the initial step, there are two possible situations: if there is, up to some small margin of error, any information about the pose of the vehicle, $Bel(x_0)$ could be initialized by samples of a narrow Gaussian centred at the right pose. If there is no knowledge about the initial state, the belief $Bel(x_0)$ can be initialized with samples of a uniform distribution normalized by $\frac{1}{m}$, being *m* the number of particles.

The more basic implementation of the Monte Carlo filter is called the *Sequential Importance Sampling (SIS) Algorithm*. It is also known as: bootstrap filtering, condensation algorithm, particle filtering, interacting particle approximations, or survival of the fittest. In essence, as each sensor measurement is obtained sequentially, the algorithm recursively propagates the weights and support points (particles). This behaviour, however, leads to the *degeneration problem*: the variance of the weights can only grow up as time increases, and so, in practice, after a few iterations of the algorithm, only one sample has an importance factor big enough to survive.

Several techniques have been proposed in order to overcome the degeneration problem of the Monte Carlo method:

1) *Selection of the importance function*: A natural solution to limit the degeneration is to choose the importance function that minimizes the variance of the importance weights.

2) *Rao-Blackwellisation for Sequential Importance Sampling*: These methods also make a decrease of the variance and are designed to reduce the number of variables that must be sampled by identifying variables that do not need to be sampled.

3) *Resampling*: The idea of the resampling methods is to deprecate those particles which have small importance weights and to concentrate in those with large weights**Errore. L'origine riferimento non è stata trovata.**. This is the method adopted in our experiments.

We now briefly describe the steps of the SIS algorithm, which will be extended in later where the integration in AGAVE is presented. The main steps of SIS are:

- **Step 1: Prediction.** Draw the set of *m* particles, where *m* is the number of samples chosen for the particle filter. This is done using the motion model of the vehicle, that is, we apply the last vehicle action to each previous particle, and thus generate the predicted prior distribution.

- **Step 2: Update.** We use an observation from a sensor to update the posterior of particles. In other words, we calculate the new weights for the particles, using the observations, like this:

$$w^{(i)}_{t} = w^{(i)}_{t-1} \cdot p(o_t \mid x_t^{(i)}) \qquad (3.2)$$

where *i* is the current particle index and *t* is the time step.

√ **Step 3: Normalization.** The new weights obtained for the particles are normalized following (3.3) in order to obtain $\sum_{i=1}^{m} w_t^{(i)} = 1$.

$$\hat{w}_t^{(i)} = \frac{w_t^{(i)}}{\sum_{i=1}^{m} w_t^{(i)}} \qquad (3.3)$$

√ **Step 4: Resampling.** To avoid the degeneration problem, a resampling step is applied. First, we find out whether it is necessary a resampling step. For that purpose, we calculate the number of effective samples, Neff, which gives us a measurement of the number of samples that are a good approximation of the belief function:

$$N_{eff} = \frac{1}{1+Var(w_t^{*(i)})} \qquad (3.4)$$

where $w_t^{*(i)}$ is the *true weight*. This value of N_{eff} cannot be calculated exactly, because the true weight value depends on $p(x_t^{(i)} \mid o_{1:t})$, but an estimate can be computed as:

$$N_{eff}^{*} = \frac{1}{\sum_{i=1}^{m} \left(w_t^{(i)}\right)^2} \qquad (3.5)$$

Now, this number of effective samples is compared with a threshold $\beta \cdot m$ established to evaluate if N_{eff} is sufficient or a resampling needs to be done:

$N_{eff} \leq \beta \cdot m$ resampling is necessary

$N_{eff} > \beta \cdot m$ resampling is unnecessary

The resampling consists of eliminating those samples which are not near the real belief function and replacing them with more accurate samples, i.e. with higher weights. The importance factors of the moved particles will also be recalculated. We have used in our experiments a value for β of 0.5.

There are several methods to make the re-sampling. Here, we have followed the scheme called, *systematic resampling* (see for implementation details).

Integration of MCL in AGAVE

The main objective of the AGAVE project is the development of an advanced guidance system for automatic guided vehicles, based in a next generation positioning system. Because of all the advantages mentioned in the previous sections, we consider the Monte Carlo method as a suitable approach for designing such positioning system. It also facilitates the fusion of different sensory data and provides a basis for considering non-gaussian-sensors, like is the case of UWB when not LOS is achievable.

The vehicles involved in the AGAVE project will derive localization from two kinds of sensors: the UWB system and the GPS equipment, so we are facing a multisensor localization problem. In this case we will talk of *Multisensor sequential particle filter (MSPF)*.

To deal with a multisensor situation we consider that:

$$p(o_t^1,...,o_t^N \mid x_t^{(i)}) = \prod_{j=1}^{N} p(o_t^j \mid x_t^{(i)}) \qquad (4.1)$$

where *N* is the number of different sensors. This modifies the update step previously depicted, as each importance factor is calculated now with the data coming from the existing sensors, so the weights expression $w^{(i)}{}_t = w^{(i)}{}_{t-1} \cdot p(o_t \mid x_t^{(i)})$ becomes:

$$w^{(i)}{}_t = w^{(i)}{}_{t-1} \cdot p(o_t^1 \mid x_t^{(i)}) \cdot p(o_t^2 \mid x_t^{(i)}) \cdot ... \cdot p(o_t^N \mid x_t^{(i)}) \qquad (4.2)$$

With this small modification, the algorithm presented earlier can be used to compute the AGV localization in a simple and efficient way.

Table 1.2 enumerates the behaviour and probabilistic models that need to be known to compute the MCL. For simulation purposes only, it is needed the *ground truth mod*el. It simulates the real movement of the AGV, not the measurements provided by the odometry. This information is unavailable in non-simulated environments (it is the one to be estimated).

MODEL	DESCRIPTION
Motion model	Probabilistic generalization of the AGV kinematics. Model of the action behaviour.
UWB sensor model	Observation model for the UWB sensors. There are two possible approaches for the behaviour of these sensors that will be presented in the next section.

GPS sensor model	Observation model for the GPS sensor. Includes both the noise performance of the sensor and the relation between measurements and position of the AGV.

Table 1.2 Models required for the integration of MCL into the AGAVE AGVs.

Sections **Errore. L'origine riferimento non è stata trovata.** and **Errore. L'origine riferimento non è stata trovata.** describe the motion model and the ground truth model respectively. The UWB and GPS sensors models will be studied in sections 0 and 0.

UWB sensor behaviour

We can consider two possible configurations of the UWB radio elements:

- **Approach A:** For the first configuration, we take into account the fact that the UWB radio stations provide only information about the distance between both sides of the communication as well as identification of themselves, that is, they act as non-ambiguous beacons. The distances provided by the beacons are nothing but sensor measurements, and so a particle filter can be applied in order to obtain the position of the vehicle. This option allows the easy integration of UWB and GPS sensors measurements and incorporates all the advantages of the particle filters into the UWB localization. We have developed several performance tests to evaluate the particle approach to positioning whose results and conclusions are presented later in this section.
- **Approach B:** On the other hand, the distance measurements can be processed to obtain information about the position of the AGV, that is, the x and y Cartesian coordinates. In this situation, it can be considered that there is only one meta-UWB sensor that gives pose information with a particular noise characterization. There are available some methods for obtaining the position from the distance, for example, in**Errore. L'origine riferimento non è stata trovata.** it is proposed the usage of a set of fixed nodes and a number of tags placed in the vehicles. The study of the performance for this kind of systems will be made in future technical reports

It is remarkable that, in both cases, no data about the vehicle orientation is considered as the current systems can't provide angle information. However, the MCL approach can be easily extended in the future to cope with that information without requiring additional equipment or processing.

Next we describe the UWB behaviour under approach A. As mentioned, approach B is left for future work.

Distance UWB sensors performance

The UWB radio system provides to the vehicle range measurements from it to N_b radio beacons located at fixed known positions. That is, we have N_b sensors that provide information of *distance* to a particle in

order to obtain the position of the vehicle. In our experiments we place the sensors evenly distributed in a circumference around the movement region of the vehicle with a radius R_b large enough to have no bias (in our experiments R_b = 10 m) and always in LOS conditions. As the sensors are not ideal, there will be errors in the data provided by the beacons. These deviations will be modelled as a Gaussian noise with mean value the real Euclidean distance between the beacon and the vehicle and a standard deviation σ_{UWB} that we have deduced from he results in. The vehicle will be following a circular path within an area surrounded by the beacons with a linear speed of 0.2 m/s and an angular speed of -π/100 rad/s, as shown in Fig.9(a).

a)

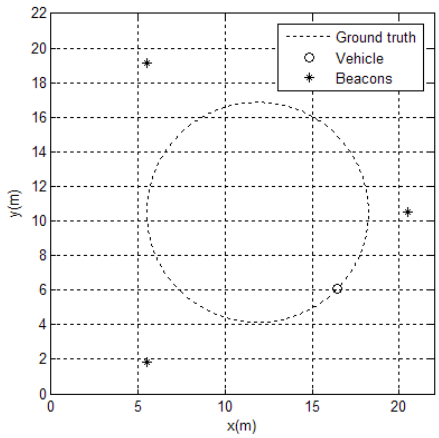

(b)

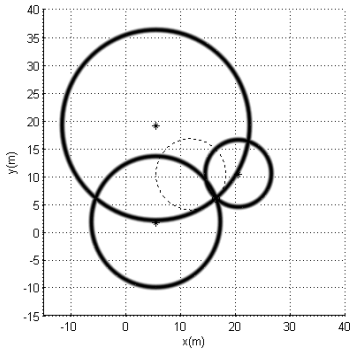

(c)

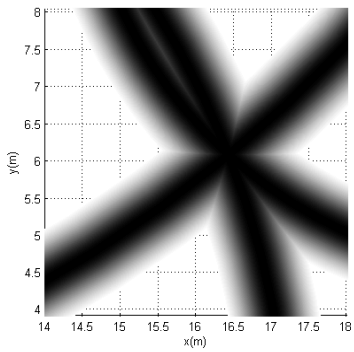

Fig. 9 Intersection of the circles of range measurements for three beacons with R_b = 10m and σ_{UWB} = 30 cm when a vehicle describes a circular trajectory. Plot (a) represents the real movement of the vehicle along the path. In (b) it is represented the intersection between the beacons distances, and in (c) we zoom in the intersection point considering range uncertainty (the darker the more likely the pose).

As it can be seen in Figure 9, due to the errors in the given distances, the intersection of the circles of the beacons determines a fuzzy area where the vehicle can be, but not a single point. This uncertainty will be further reduced by the usage of the data fusion methods explained before.

The particle filter approach uses the range measurements provided by the beacons as inputs. The performance of the algorithm depends on the accuracy of the distance data available, the number of

beacons used, and the number of particles. We have developed several experiments in order to determine the influence of each parameter:

a) UWB sensors accuracy. In this case, we have employed three beacons and a number of particles *m* = 2000. We have run 10 simulations of 400 time steps for each one, with several values of standard deviation for the UWB sensors: σ_{UWB} = 30 cm (worst accuracy for the *Ubisense* system as it is mentioned in), σ_{UWB} = 15 cm and σ_{UWB} = 3 cm (this last value is established in for the PulsON P210 radio). Fig.10 presents the mean positioning error[1] for each experiment, as well as the 95% confidence intervals for them.

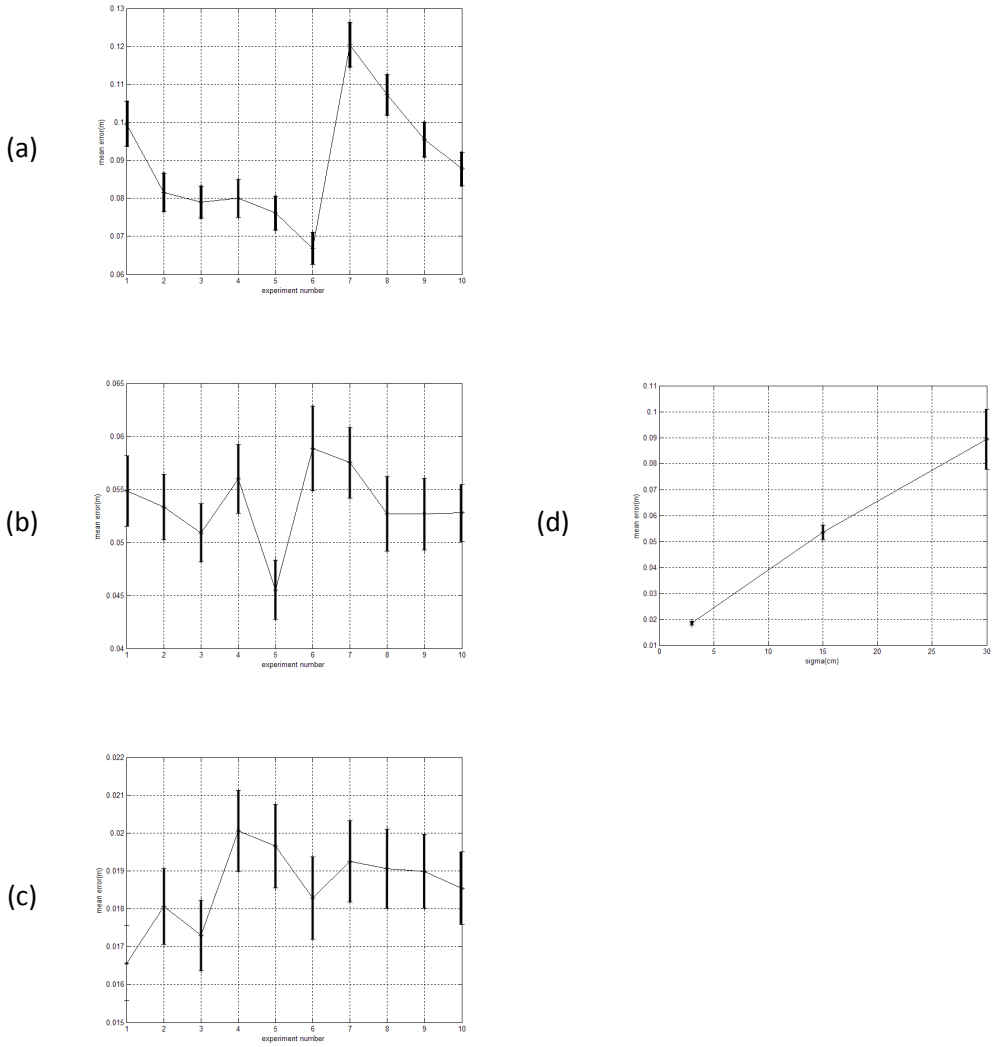

Fig. 10 Mean positioning error and confidence intervals at each time step of the experiment plotted in Fig.9 for (a) σ_{UWB} = 30 cm, (b) σ_{UWB} = 15 cm and (c) σ_{UWB} = 3 cm. Figure (d) depicts the evolution of the mean error and its 95% confidence interval vs. the value of σ_{UWB}.

[1] The error is calculated as the Euclidean distance between the position value provided by the particle filter and the ground truth position of the vehicle.

It can be seen in Figure 10 that the error obtained for σ_{UWB} = 30 cm converges to a value smaller than 13 cm; for σ_{UWB} = 15 cm, the mean error is about 5 cm and in the case of σ_{UWB} = 3 cm it is achievable an error, in the worst cases, of around 2 cm. As it was expectable, the more accurate the sensor is, the higher precision and faster convergence we get (always taking into account the degradation of performance for too accurate sensors that can be produced in particle filters). We will carry out the next tests with σ_{UWB} = 3 cm, as it is the value measured for the PulsON radios.

b) Number of particles. To determine the effect of the variation in the number of particles, we have developed a set of ten experiments with the vehicle following the same path as in Fig.9(a), three beacons with σ_{UWB} = 3 cm, and 400 time steps along a circular path. These experiments have been repeated for *m* = 20, 50, 200, 2000, and 5000 particles respectively. The obtained positioning error values are presented in Fig.11.

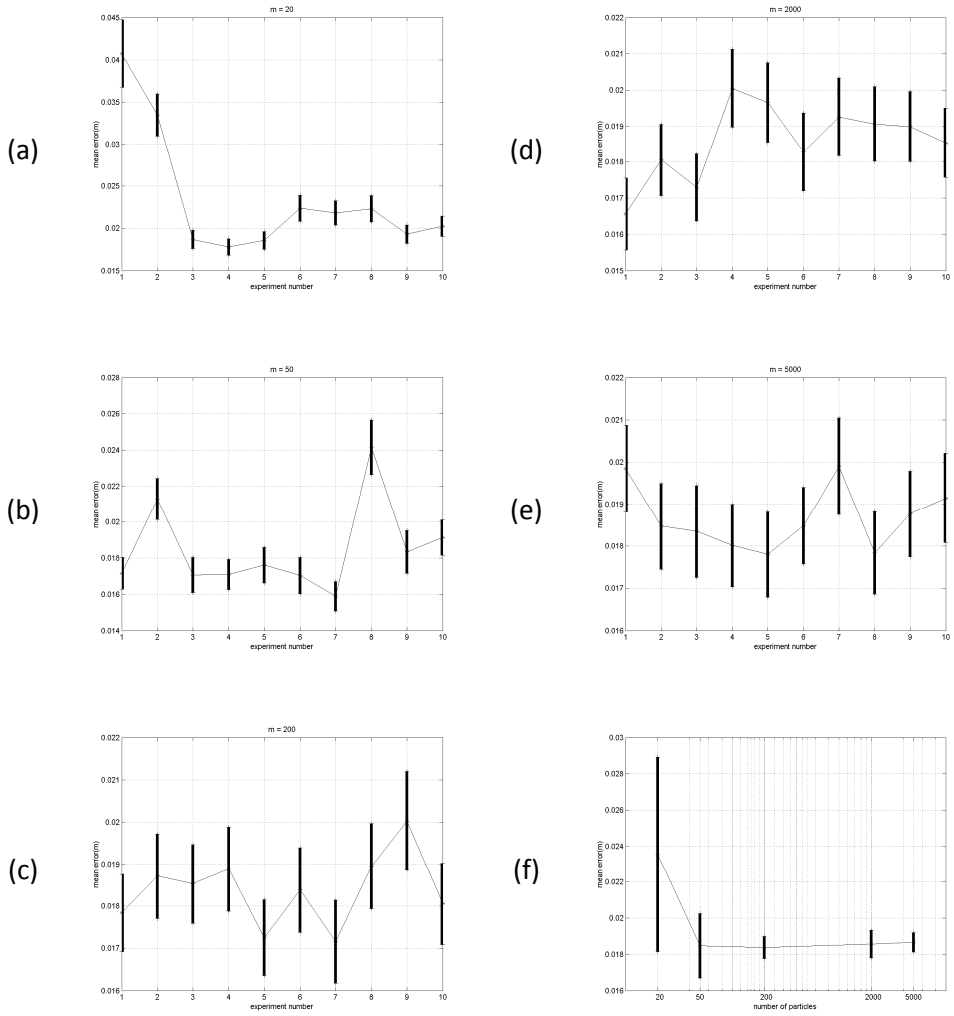

Fig. 11 Mean error and confidence intervals for the experiments realized with different numbers of particles (a) *m* = 20, (b) *m* = 50, (c) *m* = 200, (d) *m* = 2000, and (e) *m* = 5000. Figure (f) shows the evolution of the mean error and confidence intervals vs. *m*.

As it can be observed in Figure 11 the choice of the number of samples, if it is too small, affects the final performance of the system, and so *m* = 20 or 50, due to the reduced size of the particle set,

can produce results with errors peaks worse than 2 cm (see in (a) experiments 1 and 2, or (b), experiment 8). With m = 200 it is achieved a mean error smaller than 2 cm, eliminating the points above that value. The same behaviour is observable for both m = 2000 and m = 5000. In the light of these experiments, as from m = 200 the number of particles is enough, we decide to choose m = 2000 for the next tests, a size of the set large enough to guarantee the satisfaction of the convergence of the particle filter.

c) Number of sensors. We have now established a number of beacons N_b that goes from only two beacons to ten, all with σ_{UWB} = 3 cm and evenly placed at a circumference. A set of ten experiments with 400 time steps has been realized for each N_b with m = 2000, in order to assure the existence of a particle set size enough to guarantee the convergence of the MCL.

(a)

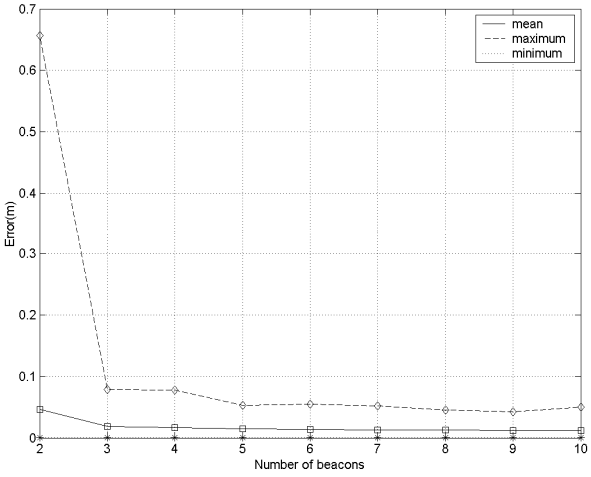

(b)

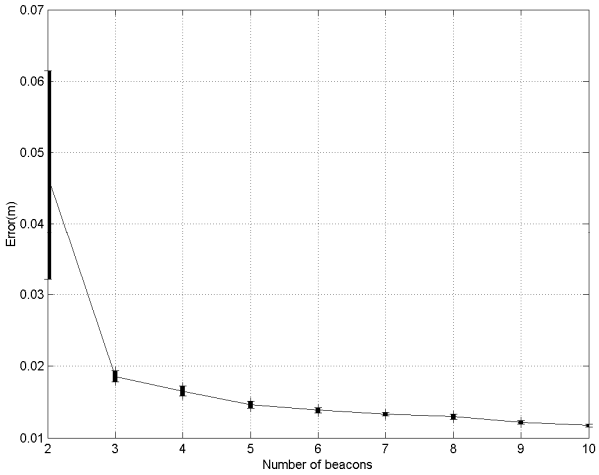

Fig. 12 Statistical parameters evolution vs. number of beacons for a mobile vehicle describing a circular trajectory. Figure (a) depicts the maximum, mean and minimum positioning error for each set of experiments and row (b) represents only the mean value with its 95% confidence intervals. The number of particles for the experiments is 2000.

The higher the number of beacons in the environment, the more accurate the system is. From 3-4 beacons and higher, good results are achieved.

The realization of these experiments permits us to say that, at least under simulation conditions, using the distances to the beacons as inputs to a particle filters:

1) The location of the vehicle can be determined with an error better than 2 cm.
2) Five beacons are enough for achieving an accuracy of 1.5 cm.

GPS sensor behaviour

The GPS sensors have been used widespread in outdoor localization of vehicles, so there are models for them accessible in literature. We will use the one presented in and model the noise of the measurements with a Gaussian distribution characterized by a covariance matrix. For example, for the Omnistar DGPS:

$$S_O = \begin{pmatrix} 0.22501 & -0.05285 & 0 \\ -0.05285 & 0.348662 & 0 \\ 0 & 0 & 0.0575 \end{pmatrix} \qquad (5.1)$$

and in the case of the Rasant system:

$$S_R = \begin{pmatrix} 0.43087 & -0.01482 & 0 \\ -0.01482 & 0.51237 & 0 \\ 0 & 0 & 0.1414 \end{pmatrix} \qquad (5.2)$$

We have used the Omnistar model to develop a simulation of localization using a particle filter with a particle number of 2000. These devices are less accurate than the UWB sensors, and so, as it can be seen in Fig.13, the results obtained are worse than the ones provided by the less accurate case of UWB, yielding a mean positioning error of 19 cm.

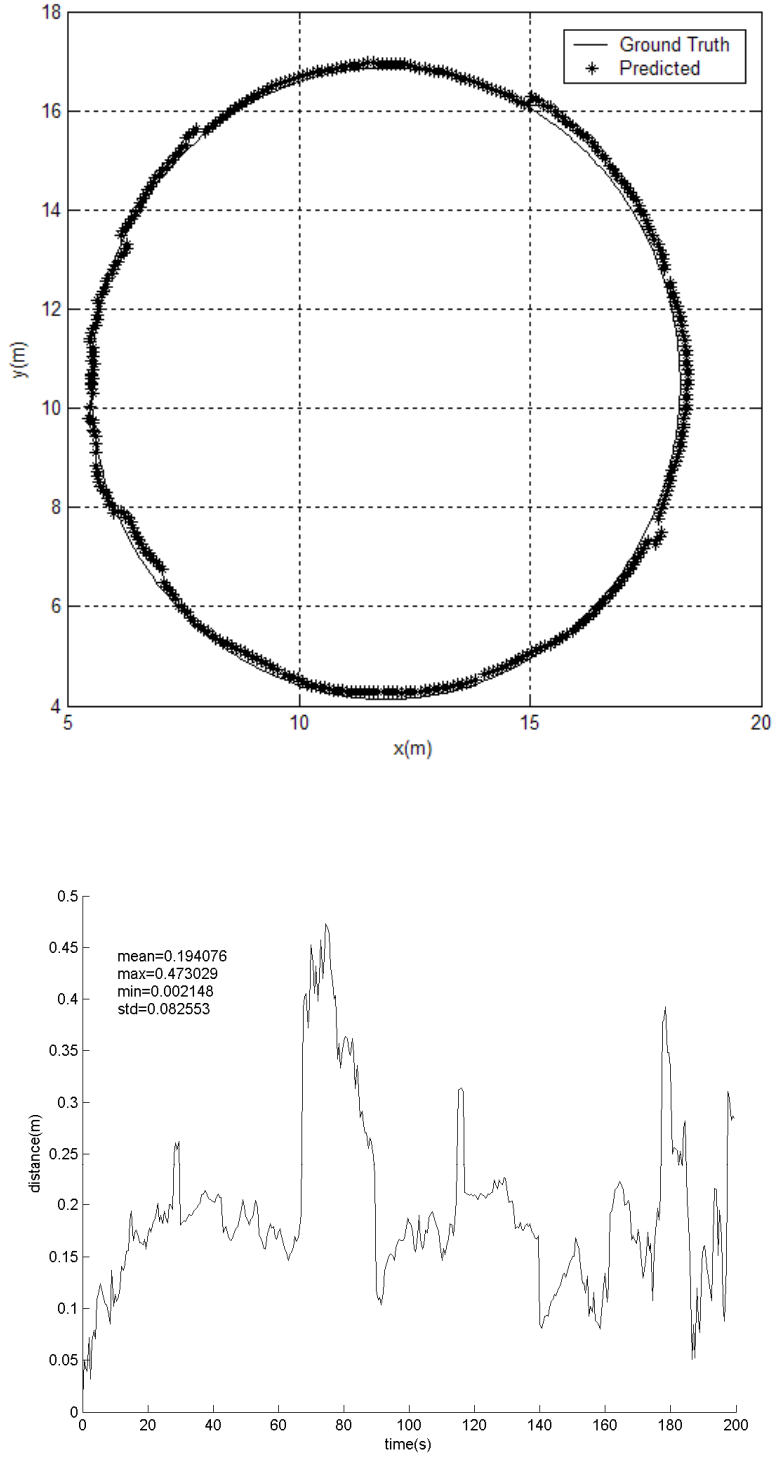

Fig. 13 Predicted trajectory vs. ground truth and action model for an Omnistar GPS sensor navigation. The upper picture presents the followed path and the estimated position with the filter and the lower the positioning error produced by MCL.

Fusion of UWB and GPS sensors. Performance of the system

Once the behaviour of each sensor has been studied separately, we integrate both systems to evaluate the performance of a system able to operate both in indoors and outdoors environments, that is, the scenario intended for AGAVE vehicles.

We develop, first, a set of experiments with a vehicle following a simple circular path. After that, a virtual warehouse environment has been built to simulate the behaviour of a vehicle operating in a plausible work scenario. These models represent a first draw of the real performance of the vehicle since no accurate UWB measurements are available yet. For that reason, these simulations should be repeated when more precise models are available.

Vehicle following a circular path

In this case, we use the configuration of Fig.9(a), but for this setting the UWB and GPS sensors will be available at alternate times: the GPS in the middle of the simulation and the UWB in both sides. This is the case, for example, where the AGV must pass trough different indoor and outdoor scenarios (a feasible situation when an AGV leaves the first floor of a factory to head for the first floor of another factory or nearby facility). In this case, it is assumed no overlapping between both devices, but our model can cope with these situations since it is prepared to work with more than one sensor. The simulation time for this experiment will be of 200 seconds (400 time steps with a sampling time of 0.5 seconds), in order to better observe the degradation of the performance when there is available only GPS information. The initial belief of the pose is a uniform distribution centred in the origin of coordinates with a maximum of 1 m. of deviation from each Cartesian coordinate of the real position, and the sensors used will be three UWB radios with σ_0 = 3 cm for UWB and an Omnistar GPS.

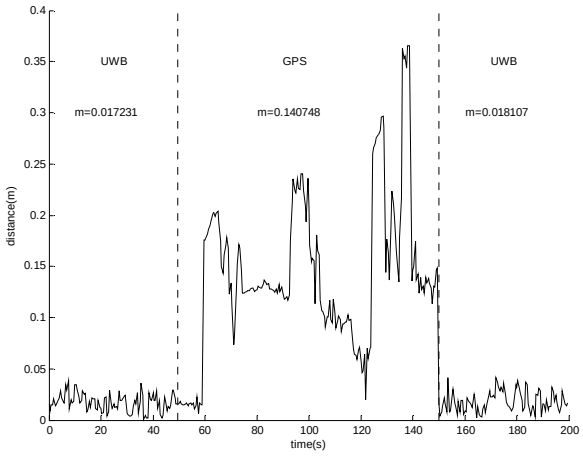

Fig. 14 Error of the MCL algorithm in the case of the alternate operation between UWB and GPS

As it can be observed in Fig.14, the error of the MCL algorithm depends on the available sensor. That is, when the UWB is turned off and only the GPS is available, there is a degeneration of the localization.

Recuperation occurs when the UWB comes alive again. It can be observed that the usage of the particle filters improves the general performance of the system by reducing the uncertainty on the position of the vehicle.

Virtual warehouse environment

Finally, we present a situation closer to the real working environment for AGAVE: a vehicle moving from one warehouse to another, for example, in order to carry a piece to a shelf. We have placed four beacons at fixed points in the walls of each warehouse. In this case, as we can observe in the figure, when the vehicle is moving through the doors, there are overlapping zones in which each of the sets of UWB beacons and the GPS sensors are providing measurements simultaneously. The UWB sensors have σ_0 = 3 cm, the GPS follows the Omnistar model and the number of particles for the filter is of 2000.

(a)

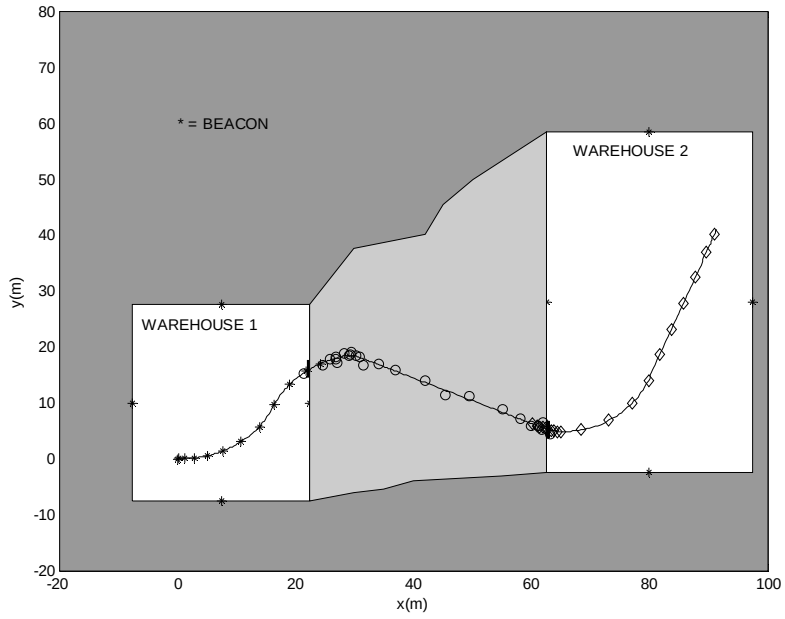

(b)

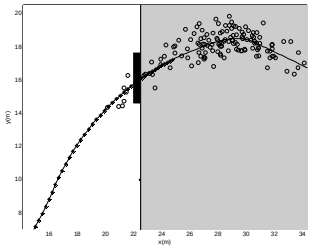

(c)

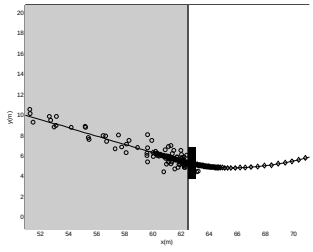

Fig. 15 Figure (a) shows sensors measurement for the path followed by the vehicles in the experiments for a real world simulation. The '*' in the walls of the warehouses are the beacons positions. The UWB beacons of the first warehouse are denoted by '*' in the vehicle path, the GPS sensor by 'º' and the UWB beacons of the second warehouse by diamonds. Figures (b) and (c) are details of the overlapping between sensors when the vehicle is passing trough the first and second doors respectively.

Now, in order to describe the simulated experiment deeply, we plot the ground truth vs. the ideal kinematical movement of the AGV and the profile of linear speed followed by the simulated vehicle.

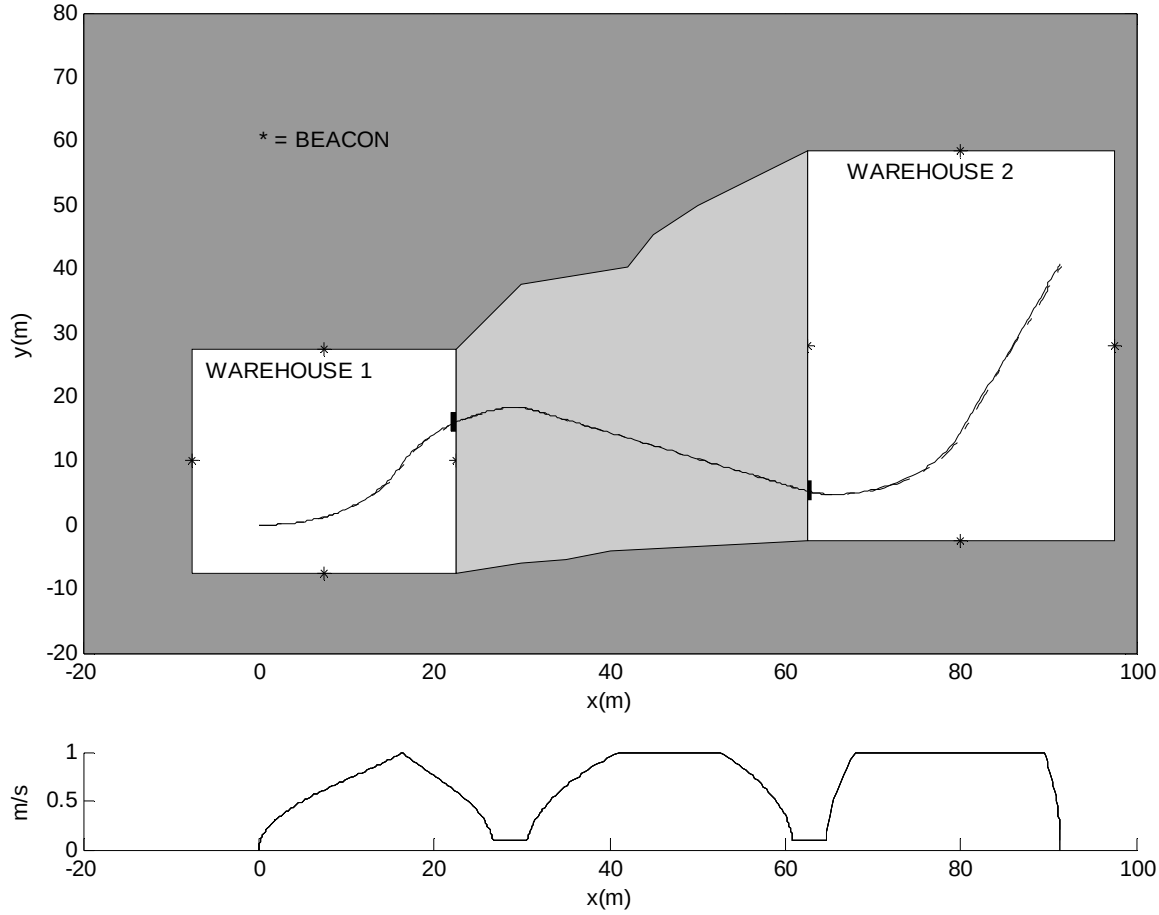

Fig. 16 Ground truth movement of the vehicle (continuous line) vs. kinematical model (dash-dot line) and linear speed profile for the experiments for a real world simulation.

The movement of the simulated AGV is slower when it is near the doors or when a turn is needed to be done, in order to reflect operation conditions closer to the real world.

In Fig. we present the position of the vehicle estimated by the particle filter, as well as the error, in terms of distance, along the path followed for the MCL algorithm.

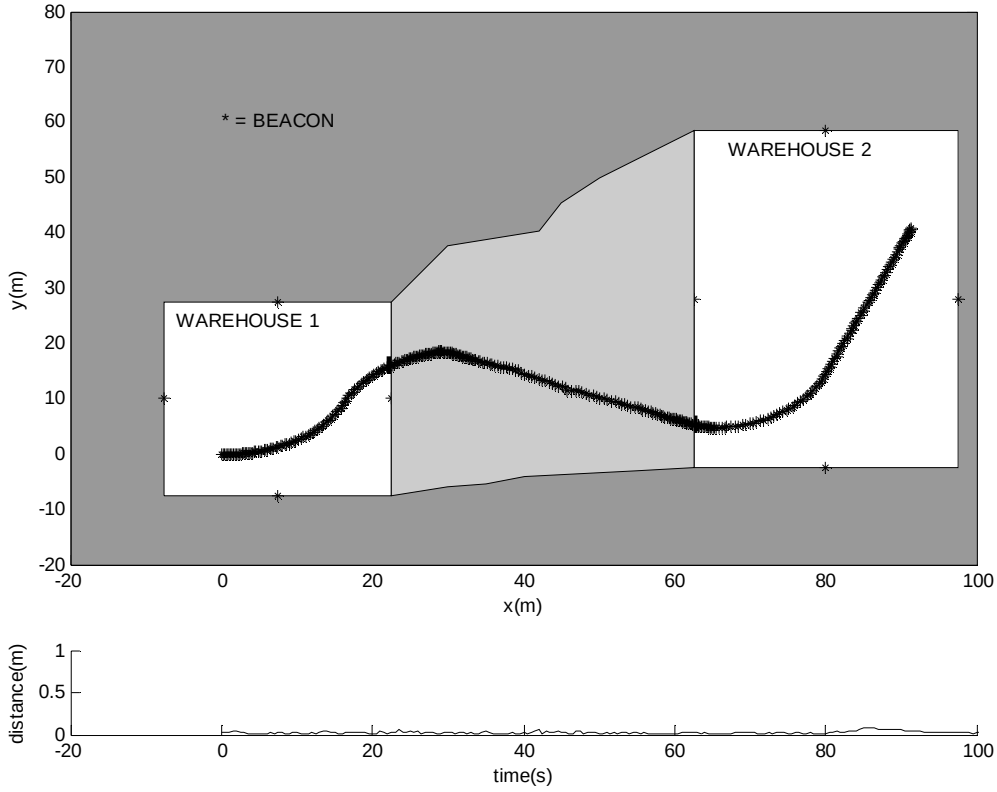

Fig. 17 Ground truth and predicted position by the MCL for a real environment simulation. The lower graph depicts the error for each time step of the simulation, as well as the mean, maximum and standard deviation of it.

1.4.3.2 Implementation of the Data Fusion technique

This section presents the results achieved when performing global localization with UWB measurements using two different data fusion techniques: Triangulation and Particle Filter (PF).

We have used the .DLL application provided by Labor (available in the attached CD-ROM) to obtain the range measurements from the UWB devices and to get the pose estimation computed by the Triangulation method.

Data Fusion Techniques Overview

In this section we outline the methods used to estimate the robot pose at each time step (k):

$x_k = (x, y, \phi)$, where x, and y are the spatial coordinates within the environment and ϕ stands for the robot orientation.

A. Triangulation (Labor's method)

This approach has been provided by Labor and yields an estimation of the robot pose from the set of UWB measurements taken at each time step. Since this estimation has not information about its uncertainty, it is not possible to fuse it with other sources of information (such as odometry).

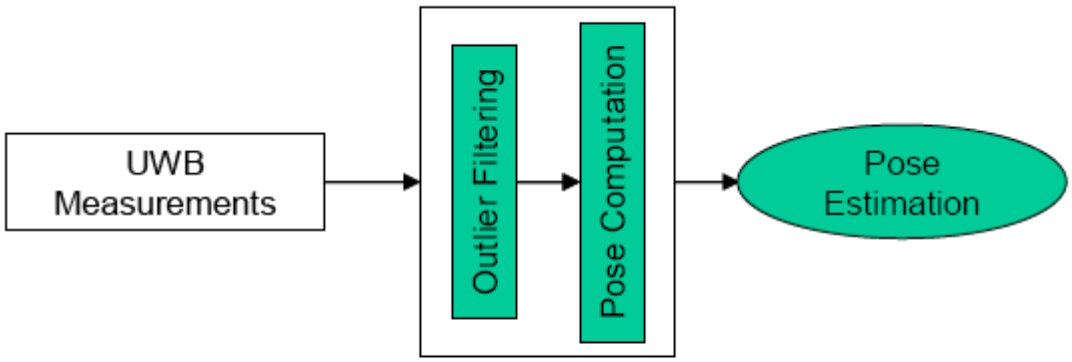

Fig. 18 – Block diagram of the Triangulation method

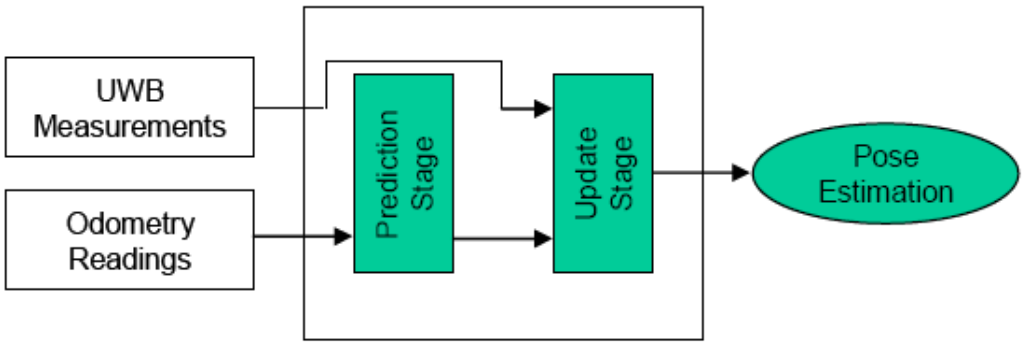

Fig. 19 – Block diagram of the Particle filter method

Fig. 18 shows a block diagram of this approach, which has been deduced from our experiences with the provided application. If any of the UWB measurement is not considered to be consistent with the rest of the measurements, it is rejected and not taken into account when estimating the robot pose. When there are less than three consistent range measurements the algorithm is not capable to perform the triangulation method yielding $x_k = (0, 0, 0)$ as the pose estimation.

B. Particle Filters (PF)

PFs are methods for implementing Bayes filters which are able to manage complex and multi-modal distributions by representing the belief in the robot pose with a set of weighted samples of its distribution.

In short, PFs algorithms can be depicted as follows (see Fig. 19):

1. Odometry readings propagate the state of the particles (prediction stage) yielding a set of particles which represents prior estimates of the robot pose.
2. The prior estimates are subsequently weighted according to the range measurements from the beacons (update stage) yielding a new set of particles which represents the posterior belief of the robot pose.

If the size of the particle set is high enough, it can be assumed that they represent properly the distribution of the robot pose estimation.

Experimental Setup

In order to perform the global localization experiment, we have arranged three UWB antennas (which will act as fixed beacons) around the navigation area. Fig. 20 shows two images of the slave UWB antennas in their fixed positions, while in Fig. 21 it is depicted a plan of the environment as well as the chosen reference system. According to this reference system, the beacons coordinates (measured by a measuring tape) are the following:

ID	X (m)	Y (m)	Z (m)
1	0	0	0.91
2	-0.32	4.33	1.37
3	3.40	2.86	2.17

We have equipped one of our mobile robots with a fourth UWB device (acting as the master) and guided it through the environment while acquiring range measurements from the beacons and odometry readings from the robot's encoders. The robot followed a circular path around the tables located in the middle of the room.

Fig. 20 - Slave UWB antennas deployment

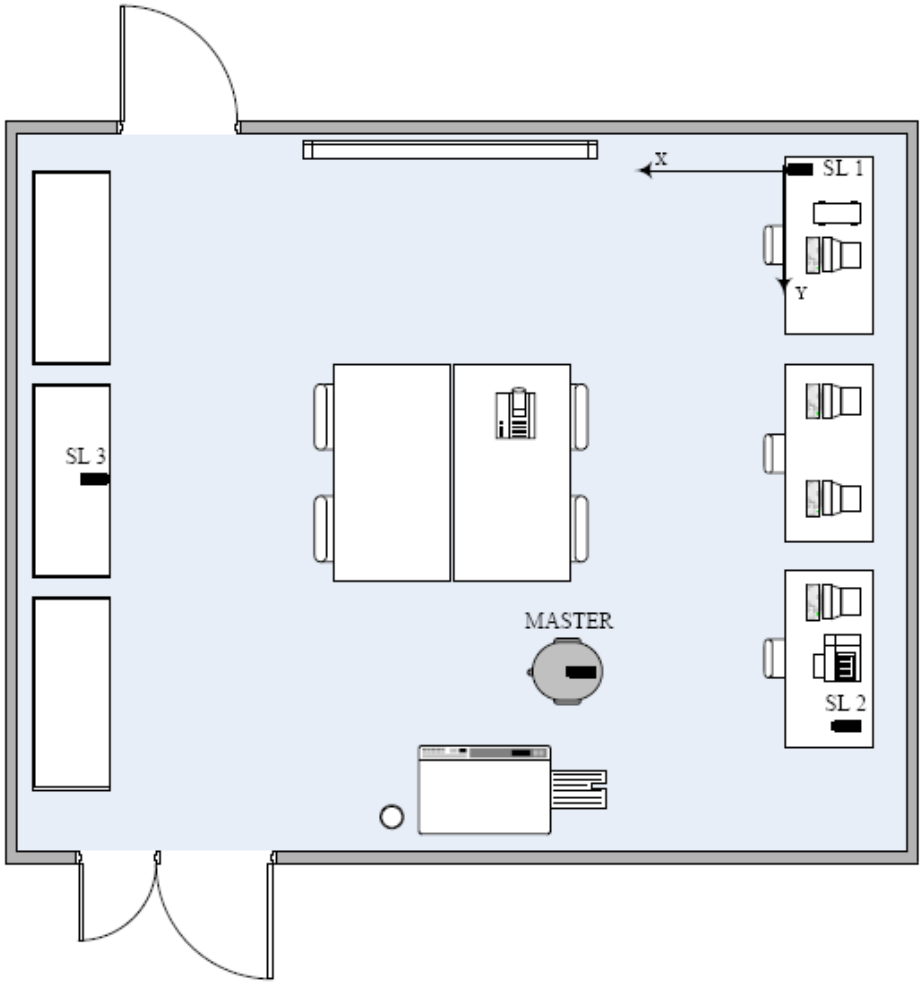

Fig. 21 - Plan of the warehouse where the experiments were performed

Experimental Results

In this section we present the results of the performed experiment where the Triangulation and Particle Filter approaches have been compared. Fig.22 shows the robot path estimated by those methods (Triangulation – green, PF – blue) as well as an estimation of the real path computed from laser scans (red).

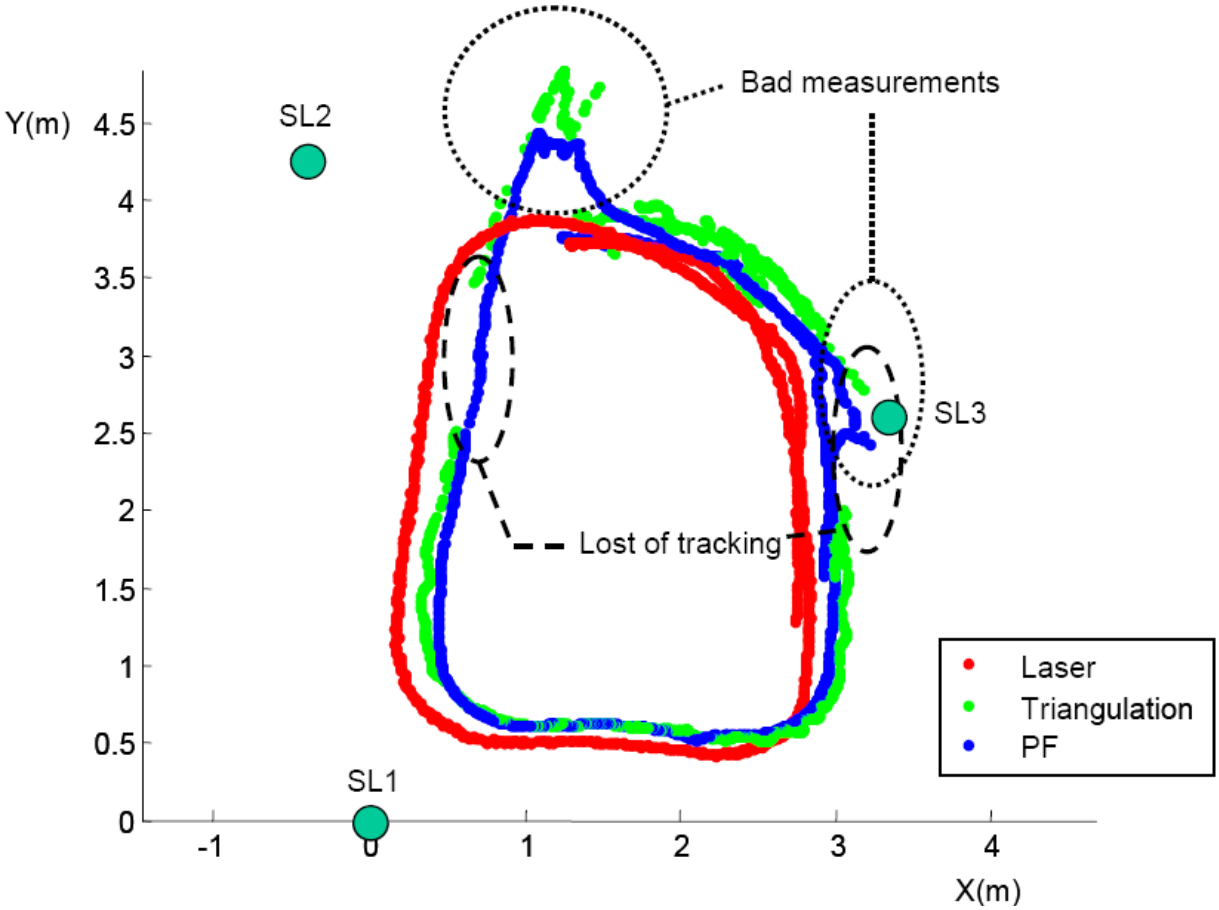

Fig. 22 - Estimated path of the robot using Triangulation (green) and Particle Filters (blue). An estimation of the real path computed from laser scans (red)

Notice that there are zones in the navigation where the Triangulation method loses the tracking of the robot due to the fact that there are less than three consistent measurements. In those zones, the Particle Filter approach uses the odometry readings to estimate the robot pose thus avoiding the lost of the tracking. Moreover, there are also zones where spurious range measurements are not properly filtered yielding a highly inaccurate estimation of the robot pose. Since those spurious measurements seem to be consistent with the robot movement, they are taken into account by the localization methods. The main causes of those transient (during several seconds) errors in the estimated range measured by the UWB devices can be interferences from nearby metal objects or the difference in height of the UWB devices positions (which would affect the measurements if the UWB antennas were not absolutely omnidirectional).

Two videos showing the whole localization experiment have been uploaded to the Groupware: Test2D.avi shows the resulting paths of the methods compared in the experiment described in sections III and IV while Test3D.avi contains a 3D animation where the UWB beacons are represented by small red spheres and their range measurements by semitransparent spheres. The set of particles are plotted as blue dots on the

ground floor, and surrounded by a red ellipse representing the spatial uncertainty. Labor's method estimation is also shown as a green dot on the ground plane.

1.4.3.3 Integration of the MEMS gyroscope

For any AGV it is a major issue that of estimating its position into the working environment. Although this task is partly carried out through external sensors, incrementally computing the ego-motion of the vehicle using proprioceptive sensors still is a fundamental step to obtain an estimation of the vehicle displacement. In this section we deal with the sensor fusion problem for the case of an AGV equipped with an odometer and an inertial sensor (a gyroscope). We address this problem rigorously through its formulation as a probabilistic estimation problem, developing an efficient solution in the form of an Extended Kalman Filter (EKF), which could be easily implemented in the low-level firmware of the platform. Experimental results reveal a qualitative improvement in the vehicle pose estimation for our sensor fusion system when compared with odometry only.

For mobile robots to become of practical utility in the industry or in the service sector, it is a fundamental prerequisite that they have a certain degree of autonomy. From the set of abilities that this implies for a robot, a remarkable one is to estimate and track its position within the operation environment, namely localization. Many practical robot tasks (e.g. navigation, picking and delivering) show up the importance of such ability. Localization is an issue extensively studied in the robotics community, where probabilistic approaches have demonstrated to be the most effective and promising ones. In those approaches a fundamental constituent is the probabilistic, incremental estimation of the robot displacement for close time steps. That is the issue addressed in this work: how to obtain an optimal estimation (under Gaussianity assumption) of the robot displacement from different ego-motion sensors on the robot.

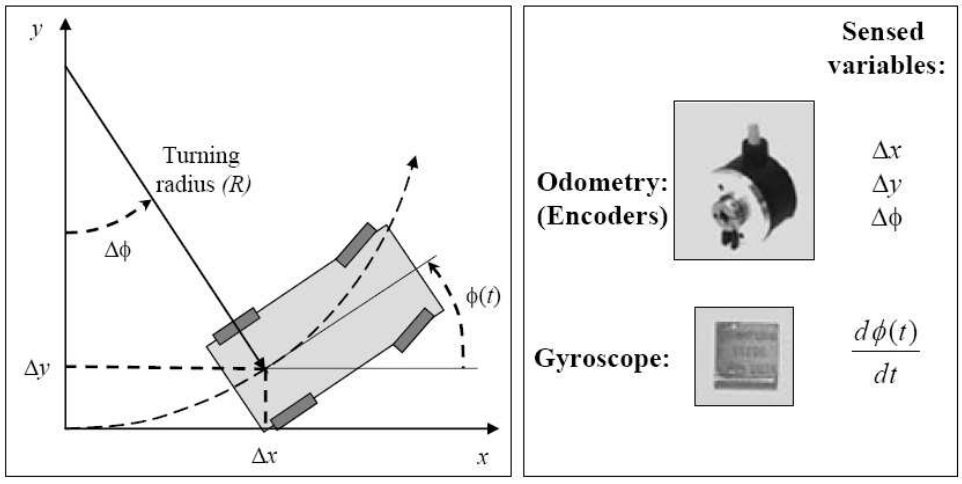

Fig. 23 - The kinematic model of a planar, differential-driven vehicle is shown on the left. The proprioceptive sensors employed in this project are visible on the right

In spite of a number of proprioceptive ego-motion sensors existing for ground mobile robots, odometers are included into virtually all commercially available ones. Actually, in most cases odometry is the only ego-motion sensor on the robot. Although other proprioceptive sensors like inertial measurement units (IMUs) may provide valuable information to the displacement estimation, they are not usually integrated into commercial robots. Our aim is to integrate different kinds of ego-motion sensors into a mathematically grounded way, concretely probabilistic Bayesian estimation, while proposing a solution efficient enough (an EKF) to be integrated into the low-level firmware onboard of a real robot. The utility of sensor fusion is revealed by noticing that different sensor weaknesses and advantages may complement to each other: typically, an odometer provides a quite precise estimation of translational movements but performs poorly when the robot turns. In turn, IMUs typically measure rotations more precisely than translations, due to the additional time integration required in the latter.

The whole system has been implemented on an ATMEGA128, a low-cost, 8-bit microcontroller from Atmel, which runs at 16MHz. In Figure 24 it is shown the prototype developed in this work, which includes two Micro-Electro-Mechanical Systems (MEMS): the already introduced gyroscope ADXRS401, and a two-axis accelerometer ADXL203, which can be used to detect the gravity vector, i.e. tilt sensing, although such issue is not addressed here. The system runs autonomously and periodically reports the EKF estimation results to a host-PC via a high-speed USB connection. This prototype has been designed with the aim of minimizing costs and weight.

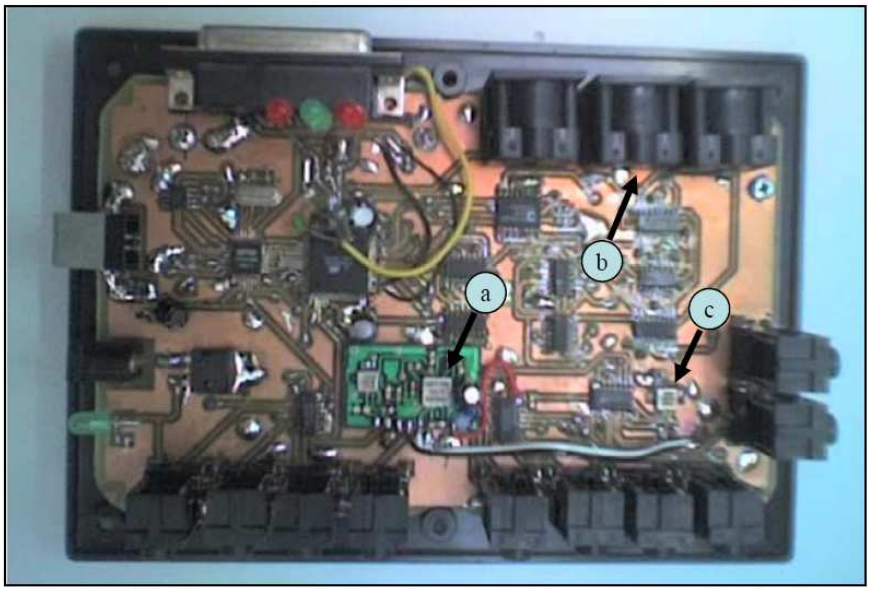

Fig. 24 The prototype used in this work as test bed for sensor fusion

Results

Two comparative experiments are reported next, where the robot follows two different paths while its pose is estimated simultaneously from odometry only, and from our sensor fusion system. The actual final robot pose for each trajectory has been determined by a highly-precise laser range scan matching algorithm 0, which we will consider the ground-truth for comparison purposes. The two different paths

consist of moving the robot on a twisty forward, and a spinning trajectory, respectively. It is noticeable the reduction in the final pose uncertainty, both in the robot position and its orientation, for the case of sensor fusion with respect to the odometry estimation only. This is numerically confirmed by the values of the covariance matrix determinant: 1.5461·10–11 from odometry only, and 2.0429 ·10–13 for sensor fusion. In the case of the spinning trajectory, the robot turns three times, which makes the odometry-only estimation to completely lose the robot orientation. The incorporation of yaw-rate information in the estimation provides an impressive qualitative improvement here: the determinant of the covariance matrix, 3.9538·10–3 for the odometry-only estimation, becomes 9.1411·10–15 for the sensor fusion case. As expected, the absolute positioning errors (relative to the ground-truth) are also reduced by the fusion of the two sensors, as summarized in Table 5.1.

	Experiment I: Forward			Experiment II: Spinning		
	x	Y	ϕ	x	y	ϕ
Odometry	4.194m	0.849m	34.42°	0.350m	0.114m	-49.55°
Sensor fusion	4.187m	0.934m	25.32°	0.096m	0.233m	2.65°
Ground truth	**4.169m**	**1.031m**	**25.80°**	**0.072m**	**0.282m**	**2.50°**

Table 5.1: Review of experimental results: final estimated pose from each method.

1.4.4 System prototyping and installation

The block diagram of the final prototype with all the implemented features and the version realised at Nuovafima are shown in the next pictures.

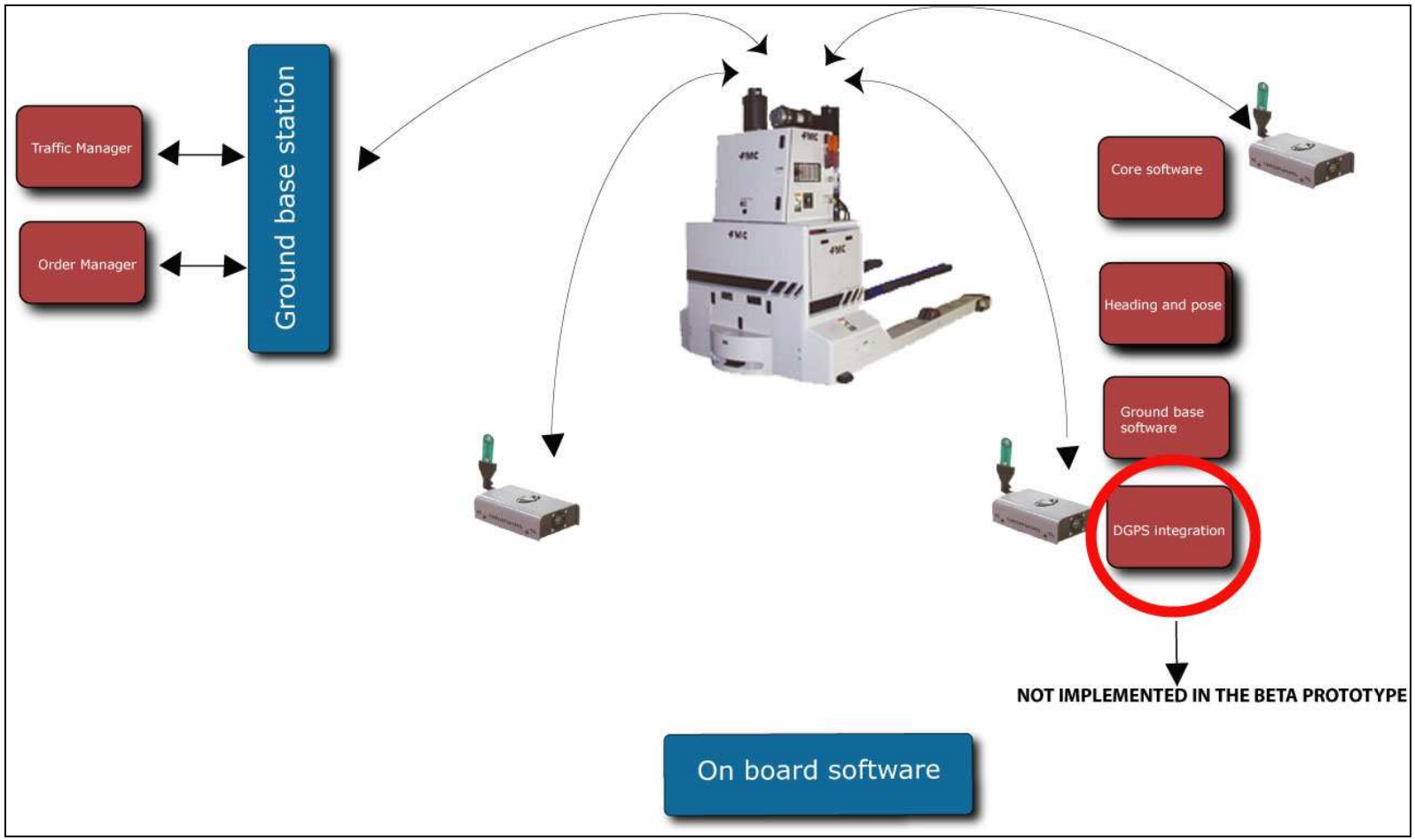

Figure 25 – Block diagram of the Beta prototype

Figure 26 – Detail of the Beta prototype

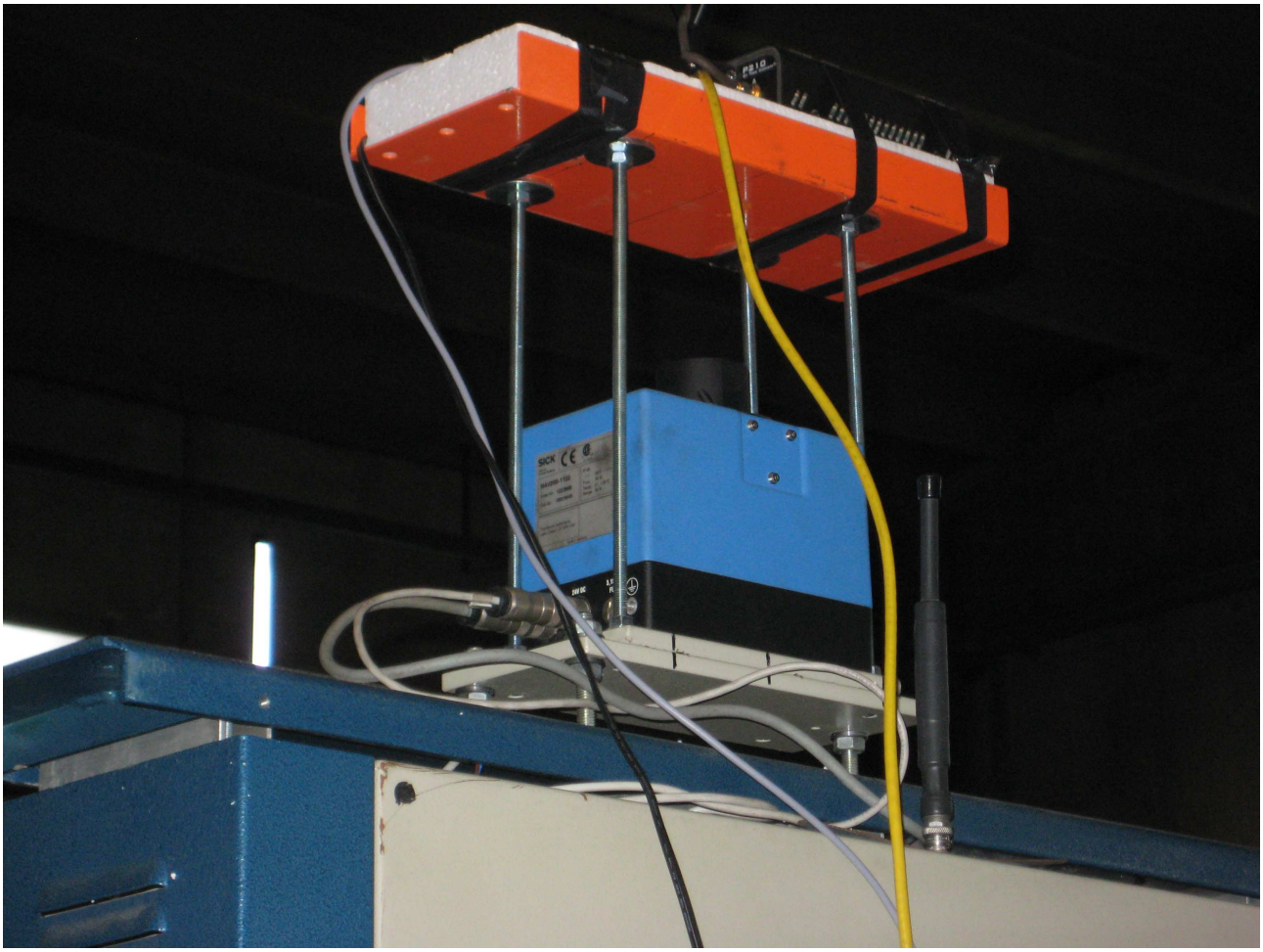

Figure 27 – The Laser Head and the UWB module

Figure 28 – The AGV, the testing warehouse and AGAVE's working group

Improvements to the Alpha prototype

With respect to the comparative tests performed on the Alpha prototype, the final Beta prototype implemented some significative changes and improvements:

1. The implementation of the MTi accelerometer, used for the calculation of the bearing and attitude of the vehicle. This was made necessary by the need to keep track of the bearing of the AGV, since Laser intrinsically provides this feature while UWB technology requires some additional hardware to be installed (either a couple of antennas, with related additional algorithms to evaluate the angle form distance measurements, or a three axial accelerometer).

   In order to ensure an optimal trade off between technical performance and cost, we chose to implement a MEMS gyroscope manufactured by Xsense, capable of determining the attitude of the vehicle with an error within 0.1'.

2. The MTi gyroscope also provides an additional input to the data fusion block, containing information on the instantaneous position of the AGV. This value is obtained by double integrating the 3D acceleration data, with output values strongly affected by errors.

Test in house

The field tests of the Beta prototype have been carried out at Nuovafima premises, in an area of 20m x 22m. Blueprints of the warehouse are available at Nuovafima. The vehicle has both the laser head unit and the UWB positioning module installed on board, stacked one above the other.

Beacons position

The position of the beacons has been determined by a surveyor, with an accuracy of ± 1mm:

beacon	X	Y
0	9.076	14.360
1	2.070	0.320
2	8.542	0.826
3	17.120	0.760
4	0.332	3.823
5	0.844	10.521
6	0.378	14.792
7	0.380	20.566
8	4.053	22.016
9	9.896	21.793
10	15.771	21.961
11	17.078	18.138

Table 1 –Beacons coordinates in the warehouse

Figure 30 –Beacons position in the warehouse (in red the laser beacons, in yellow UWB modules)

Accuracy assessment

To assess the accuracy of the measurements, the following layout has been defined:

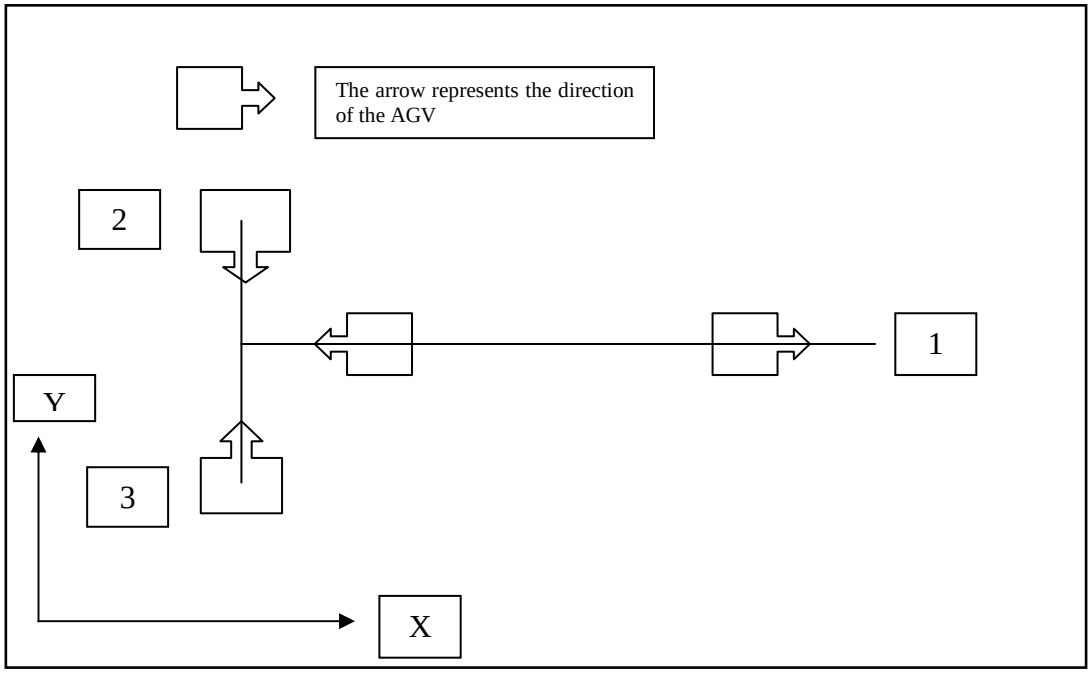

Figure 31 – The path followed by the AGV during the tests

Test is performed through the following steps:

A. AGV goes to station 1

B. AGV goes to station 2

C. AGV goes back to station 1

D. AGV goes to station 3

Test results

First set of tests: Driving with laser and position measurement with UWB

During this test, the AGV has been driven by the classic Laser system, while the complete AGAVE system has been used to compare its positioning capabilities with the standard laser system.

Results are shown in the following picture, where it is clearly visible that, although some ringing is present, especially in UWB X coordinate determination, standard deviation and accuracy values are very encouraging, taking also into consideration the limited number of beacons.

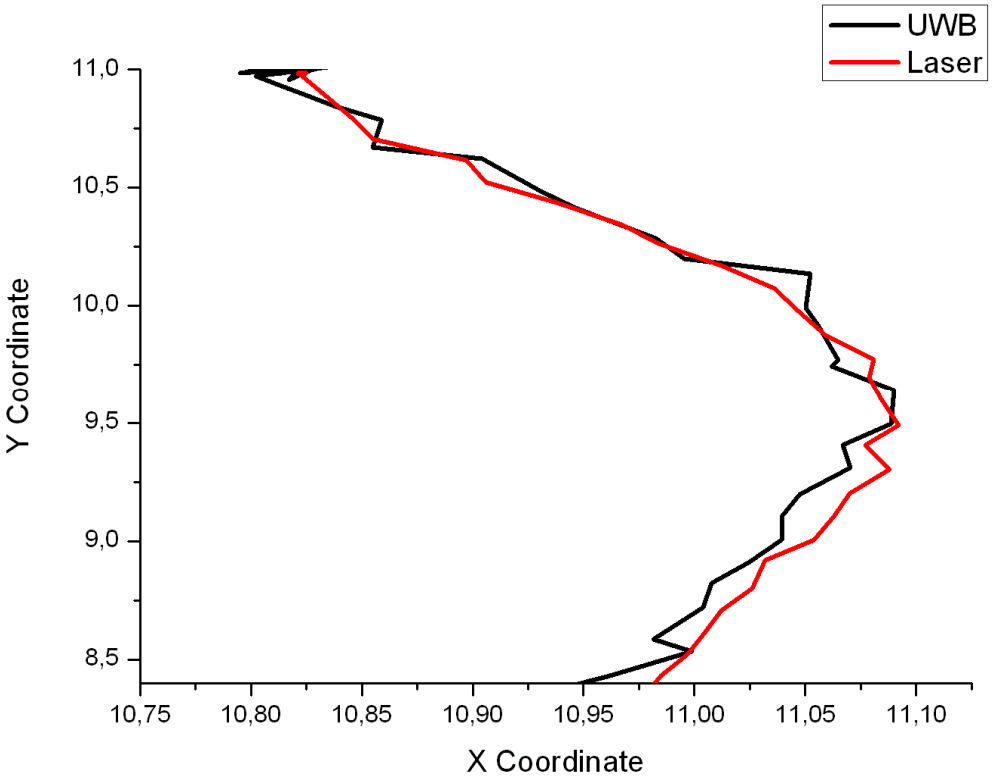

Figure 32 – The trajectory of the AGV

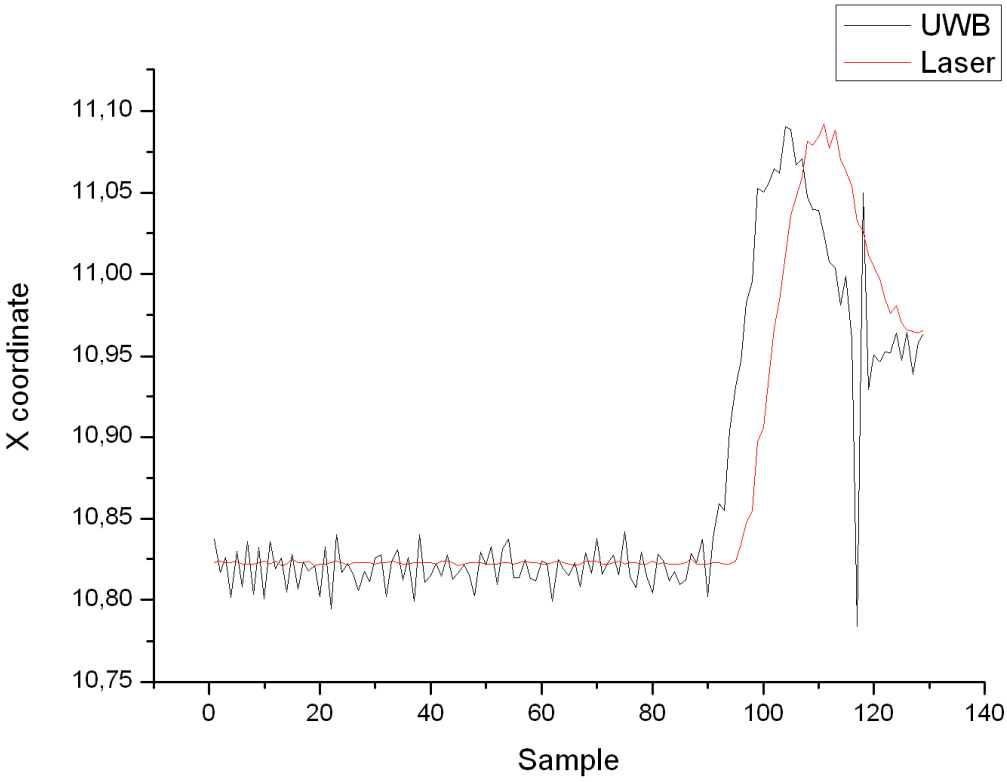

Figure 33 – Determination of the X coordinate with UWB (black) and Laser (red)

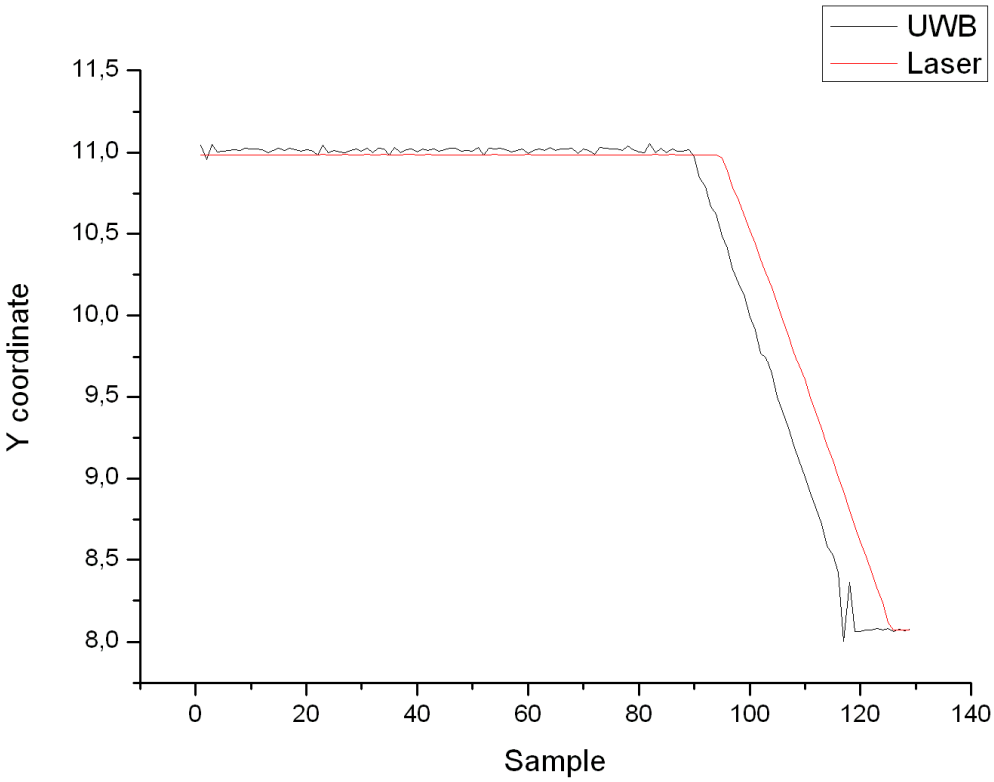

Figure 34 – Determination of the Y coordinate with UWB (black) and Laser (red)

Mean	Standard Deviation	Standard Error	Lower Confidence Interval of the Mean	Upper Confidence Interval of the Mean	
-0,08426	0,96703	0,08514	-0,25273	0,08421	
-0,1113	0,24462	0,02154	-0,15392	-0,06868	
25th Percentile	**75th Percentile**	**Inter Quartile Range**	**User Defined Percentile**	**Median**	**Variance**
-0,01554	0,0067	0,02224	0,12257	-0,00519	0,93515
-0,16899	0,03473	0,20372	0,04663	0,02257	0,05984

Figure 35 – Statistical analysis of the data: first row represents X coordinate, second row represents Y

Besides, in the following picture, the comparison between bearing and attitude measurements calculated with laser technology and the values obtained with AGAVE system, exploiting a three axes MEMS gyroscope with magnetic correction, is shown. It is evident that our system can be reasonably used in an industrial environment, providing accurate and reliable measurements, as testified by the following pictures including a statistical analysis.

The most important source of error is a constant bias due to the lack of accurate calibration before the test was started, but this has been duly corrected in the following tests.

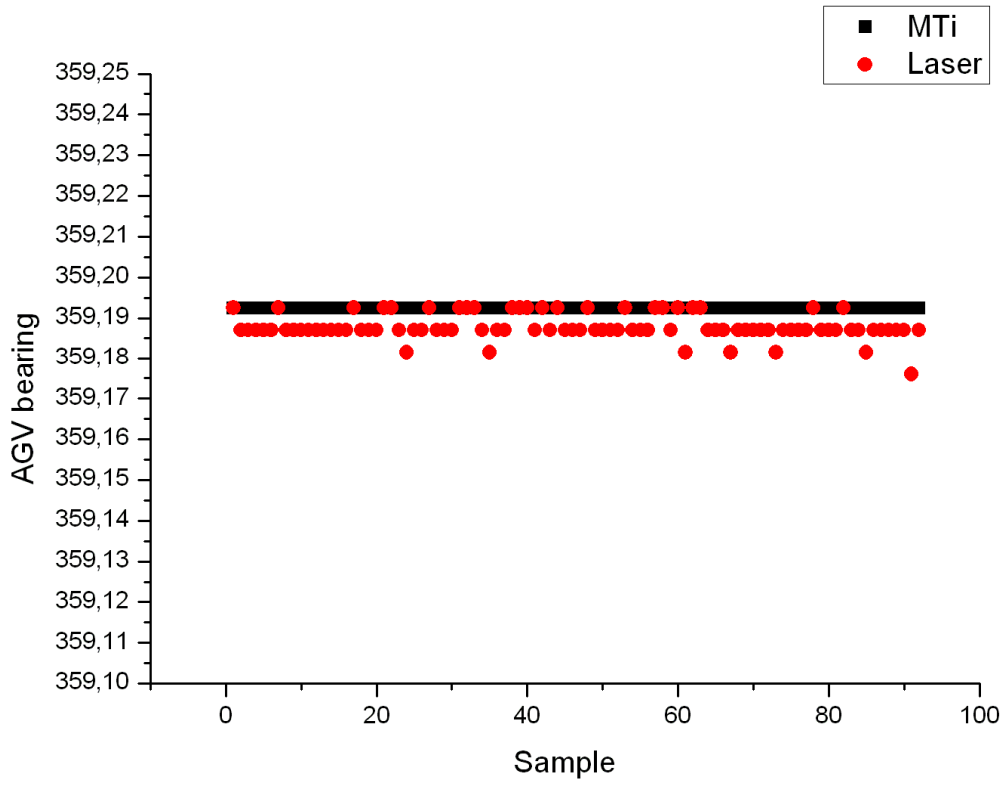

Figure 36 – Vehicle's bearing calculated with Laser (black) and with MTi (red)

Mean	Standard Deviation	Standard Error	Lower Confidence Interval of the Mean	Upper Confidence Interval of the Mean
359,1925	0	0	359,1925	359,1925
359,18796	0,0032	3,32E-04	359,1873	359,18862

25th Percentile	75th Percentile	Inter Quartile Range	User Defined Percentile	Median	Variance
359,1925	359,1925	0	359,1925	359,1925	0
359,18701	359,1925	0,00549	359,1925	359,18701	1,02E-05

Figure 37 – Statistical analysis of data relating to AGV's attitude: first row represents Laser values, second rows MTi's

Third set of tests: Driving with UWB and position measurement with Laser, with improvements to the communication protocol

This test has been run taking into account the results of previous experiments, useful to correct the communication protocol between AGAVE's laptop and the onboard PC104. These allowed a better control of the AGV, resulting in the almost seamless integration between AGAVE system and the existing hardware.

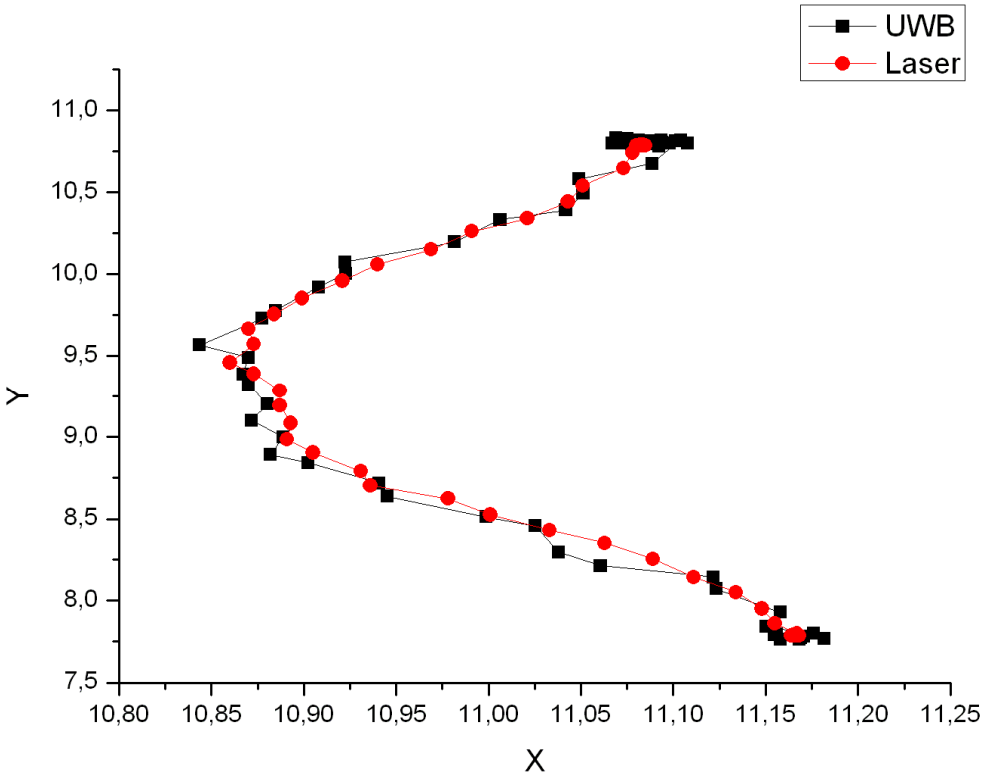

Figure 38 – Trajectory of the AGV

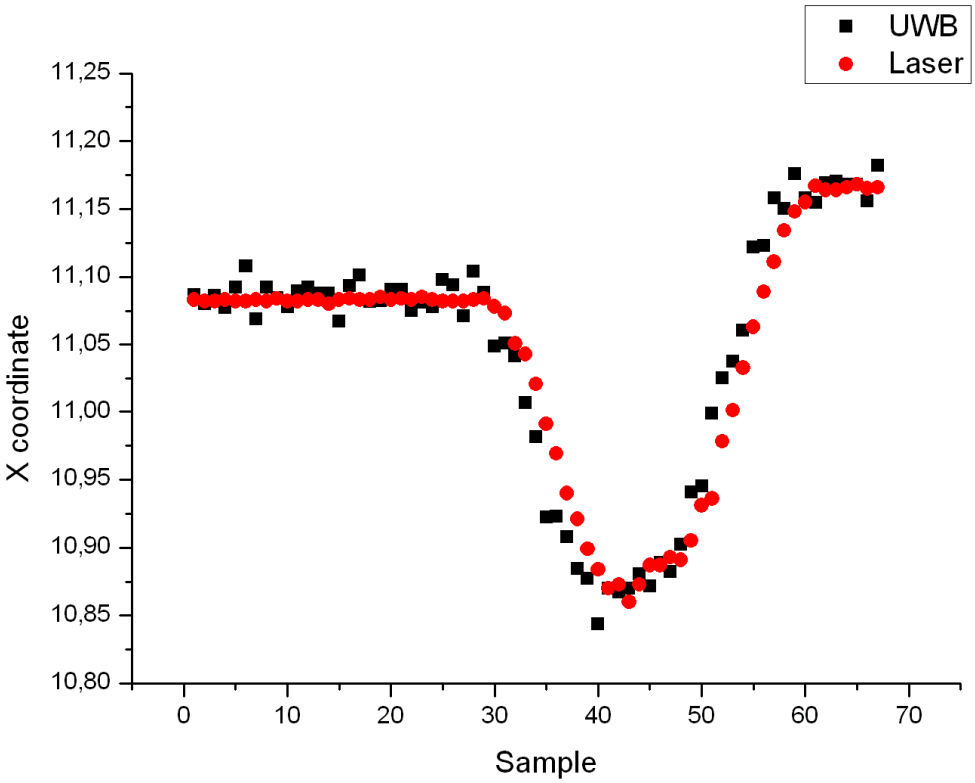

Figure 39 – Determination of the X coordinate with UWB (black) and Laser (red)

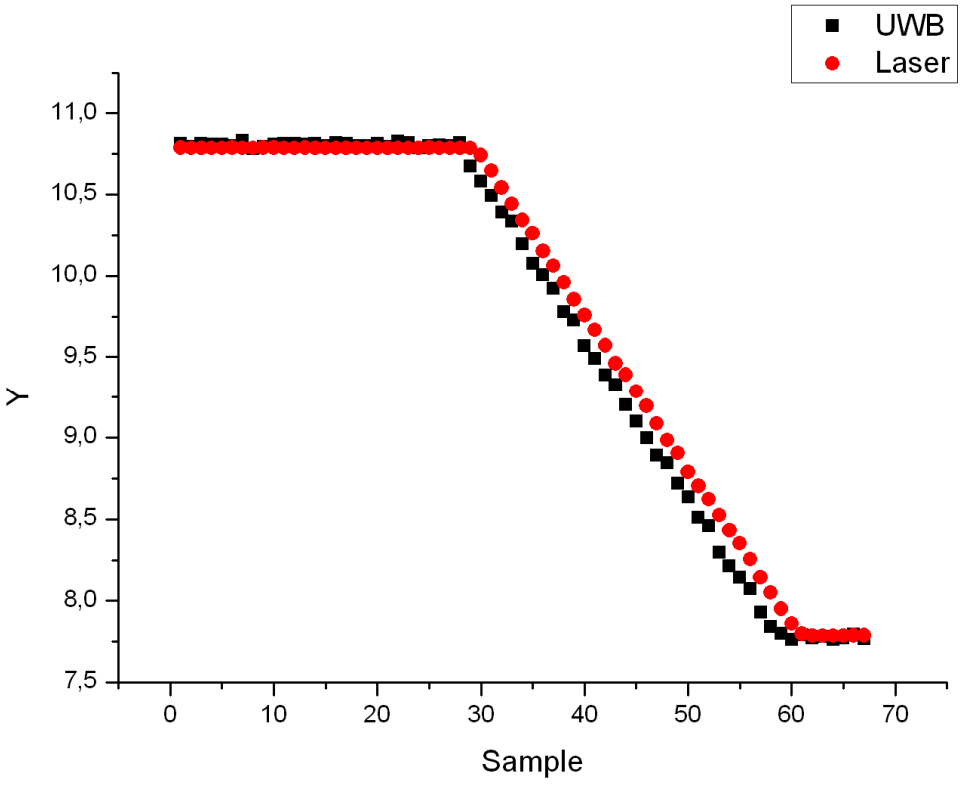

Figure 40 – Determination of the Y coordinate with UWB (black) and Laser (red)

Figure 41 – Statistical analysis of the data: first row represents X coordinate, second row represents Y

Mean	Standard Deviation	Standard Error	Lower Confidence Interval of the Mean	Upper Confidence Interval of the Mean	
0,00212	0,02383	0,00291	-0,00369	0,00794	
-0,07341	0,09577	1,17E-02	-0,09677	-0,05005	
25th Percentile	75th Percentile	Inter Quartile Range	User Defined Percentile	Median	Variance
-0,00917	0,01185	0,02101	0,04701	0,00371	5,68E-04
-0,17722	0,01822	0,19543	0,03354	-0,0216	9,17E-03

Test results

The Beta testing on the prototype defined the characteristics and operative performances of the final system, allowing further R&D activities in order to refine the product and make it available for the launch on the market likely during summer 2009.

As for the technical performances, it was important to show how the final system behaves in standard industrial warehouses and the effective added value brought about, in terms of accuracy, reliability and increased coverage in areas where laser is not applicable.

Thanks to the data fusion algorithm and the positioning algorithm implemented, AGAVE is able to ensure reliable data even in noisy environments, well beyond the native performances of the selected UWB Time Domain kits (around 30 cm in 2D positioning against 5-10 cm ensured by AGAVE as it is now).

It is important to underline that measurements have been obtained in the minimum possible configuration for a positioning architecture, namely made up of three fixed beacons and a mobile sensor; this architecture is simple, low cost but highly prone to produce invalid measurements because the inaccurate value coming from one of the fixed beacon can not be corrected by redundant measurements, turning into an erroneous positioning value.

This can be easily amended, by deploying at least 4 fixed beacons every 100 m^2; this, in turn, brings us to the economic feasibility issues, discussed in Deliverable D13, aiming at minimise the overall system costs keeping high the technical performances.

Another important issue to keep into consideration is the necessity to upgrade the navigation hardware, that now is based on a PC104 platform with an old MS DOS system running on it; AGAVE system requires a modern pc on which the algorithms (for Data Fusion and positioning)§ run, and at this stage it is impossible to implement this software on board. As a consequence, we are forced to implement a laptop on the AGV, but everything will be more compact if the PC104 was replaced with a modern computer. This, in turn, will have repercussions on the quality of the navigation software installed on board.

Another important issue to remark is that the integration with DGPS has been arranged, but due to the high costs of the equipment and the need to devote all the available resources to the system engineering phase, it has been decided not to purchase the equipment but to set up all the necessary software modules in order to allow a simple “plug and play approach” once the GPS is available.

Besides, University of Malaga carried out extensive studies and simulations on the application of UWB and GPS technologies for vehicle localisation in combined indoor-outdoor environments, in order to assess the contribution of GPS coordinates on the data fusion algorithm.

Finally, IAITI introduced several upgrades to the existing ground base navigation software, providing new and improved anti-deadlock, best route selection and queue management algorithms, ready to be implemented in the management software.

SECTION 2 Dissemination and use

2.1 *Description of exploitable results*

Exploitable Knowledge (description)	Exploitable product(s) or measure(s)	Sector(s) of application	Timetable for commercial use	Patents or other IPR protection	Owner & Other Partner(s) involved
All in one integrated system for vehicle guidance	AGV prototype	Automation	Few months after project completion	To be defined if applicable	SMEPs
Localization system and algorithms	Localization system and algorithms	Automation	Few months after project completion	To be defined if applicable	SMEPs

2.1.1 All in one integrated system for vehicle guidance

2.1.1.1 Description of result

Automatic Guided Vehicles (AGV) are designed to perform their operations without direct human guidance. They are used in a wide variety of industrial applications and usually can be laser, inertially or Cartesian-guided.

An automatic guided vehicle system, (or AGVS) consists of one or more computer-controlled wheel based load carriers (normally battery-powered) that runs on the plant floor (or if outdoors on a paved area) without the need for an onboard operator or driver. AGVs have defined paths or areas within which or over which they can navigate.

The aim of this project is to provide a new guidance system based on Ultra Wide Band technology, thus overcoming the main constraints of the classic guidance methodologies, such as the impossibility to drive a vehicle in Non Line of Sight Conditions or the inadequacy of the laser in harsh environments.

The main breakthrough will be the possibility to drive an AGV in narrow aisles or, more in general, in NLOS conditions, without the need of installing a lot of beacons, exploiting the features of UWB technology that, thanks to the spread frequency spectrum of the emitted pulses, allows the penetration of the obstacles, showing a positioning accuracy both in navigation and in docking of about 1 cm.

Another important improvement of our AGV is the statistical error correction and data fusion technique based on Monte Carlo particle filter, that allows multiple inputs (Odometry, DGPS, UWB, gyroscope for bearing and attitude determination) to feed the on board pc, giving a more reliable estimation of vehicle's position.

Moreover the classic ground base software, used to deliver to the vehicles orders and missions, will be upgraded by means of novel algorithm for:

- Deadlock prevention
- Optimal route selection

Our Automated Guided Vehicles (AGVs) deliver maximum return on investment (ROI) by reducing labour and material costs while improving safety and equipment damage.

2.1.1.2 Possible exploitation

Automated Guided Vehicles can be the best horizontal transportation method for material handling in many applications.
Summarized on this page are the benefits of AGV Systems and the situations in which they are the best solution.

- √ **Low to Medium Throughput** - In applications where the throughput relative to the distances traveled are in the low to medium range and do not warrant fixed path conveyor [25-100 loads per hour], an AGV system should be considered. Very low throughput can be best served with a manual delivery method such as fork lift trucks, while high throughput requirements are better suited for conveyor or towline.
- √ **Zone containment of manual forklifts** - Lifting stacking, and loading are functions best accommodated by manual forklift trucks. AGVs are better suited for horizontal transportation. In a properly designed system, forklift trucks are contained to specific areas of a facility [i.e. shipping

dock or staging areas]. An orderly systemized facility will not allow random disbursement of manual fork lift trucks over long distances.

- √ **Consistent and stable loads** - Applications where the load profile is relatively consistent are well suited for an AGV system. A common load footprint, which allows repeat interface by an AGV is a fundamental requirement.
- √ **Long distances** - The distance between load pickup and delivery points will influence the material delivery system solution. AGV Systems are typically favored in applications where distances between stations are approximately 200 feet or more. However, shorter distances can be justified if the vehicles are used as a bridge between two points.
- √ **Steady and continuous throughput** - In applications where material delivery requirements are steady, continuous, and repetitive shift after shift, AGVs can be the best solution. AGVs can respond well to steady, continuous flow because AGVs operate at fixed speeds and fixed operating cycles.
- √ **Electronic Dispatching of Loads** - Efficient scheduling and movement of loads can be accomplished with AGVs. Load movement scheduling can be queued in an efficient pre established manner [FIFO or prioritization]. AGVs can respond to calls for pickup and delivery; this improves material handling efficiency.
- √ **Process Automation** - AGVs can be the best solution when scheduled material flow is required in to and out of manufacturing cells. Automated manufacturing and production systems operate most efficiently when tied together by an Automated Guided Vehicles.
- √ **Sortation** - AGVs provide an excellent horizontal transportation medium when many pickup and delivery points are required. AGVs have an advantage over a conveyor solution in these situations due to the complexity and cost of the latter solution
- √ **Need For Flexibility** - If system expansion and system changes are anticipated, an AGV system may be the best solution. AGVs are more adaptable to change compared to other horizontal transportation methods such as towline, monorail or conveyor.
- √ **AS / RS Interface** - AGVs offer an excellent transportation method when load movement in to and out of an AS / RS is required. AGVs scan interface at multiple storage aisle P / D points while keeping the interface points free of a fixed obstruction. AGVs also blend well with AS / RS because both are automated computer controlled systems. A manufacturing cell can request a load to be delivered out of storage to a station. The partnership between the AS / RS and the AGV allows for combined automated storage and horizontal transportation.

Below a list of the main benefits derived from the use of an AGV system.

- √ **Improved Response Time** - AGVs can improve the material delivery response time required to a manufacturing cell or shipping dock. AGVs remove and supply loads precisely upon demand [fork trucks are undesirable for precise timing].

Safe Vehicle Movement - AGVs move slower than manually operated industrial vehicles, operate on a fixed path, and have safety features built in for pedestrian interaction. In applications where "fork truck madness" and pedestrian safety are problems, an Automated Guided Vehicle System can be a good solution. AGVs efficiently share aisles with people and fork truck traffic.

Reduction in Labor - Once set up and configured AGVs can deliver material automatically, 24 / 7, with minimal operator involvement. Therefore, material handling labor costs can be drastically reduced.

- √ **Elimination of Conveyor Walls** - AGV Systems allow open aisle ways. Since AGVs are operator less industrial vehicles, no fixed obstructions are required. AGVs are a good solution in contrast to a conveyor when a fixed obstruction is in the proposed material path. **Service From Palletizers** - AGVs are adaptable to an interface with palletizers. Since palletizers generate consistent unitized loads at a steady rate, AGVs are well suited. AGVs make an excellent bridge between the out feed conveyor of a palletizer and a storage system or shipping dock.
- √ **Eliminate Single Point Failures** - AGVS are continuous flow devices. However, AGVs are almost immune to single point failures, which could occur on conveyors or monorail systems. One AGV may malfunction but other vehicles will continue to deliver material during its repair. If a vehicle fails on a main guide path, it can be easily moved, allowing for material flow to continue unabated.
- √ **Adaptable to Manual Backup Methods** - An AGV system allows open aisles and open accessibility to pickup and delivery points. If the AGV system is inoperative, loads can still be delivered by a manual method, such as forklift truck.
- √ **Reusable Asset** - An AGV System is an reusable asset to any facility. An entire AGV System can be moved to another location or another plant with minimal downtime. Vehicles, Batteries, Chargers, and Fixed Controls can also be moved easily. The only system elements than cannot be reused are any in-floor guide wires.
- √ **Reduced Product Damage** - AGVs move slower and are in general more careful than manually operated fork trucks. Therefore, AGVs allow little or no product damage in comparison to fork trucks.
- √ **Better Tracking of Materials** - AGV control systems allow tracking of materials while loads are in the AGV system. Each pallet can be uniquely identified and tracked throughout the material transport process. In addition, load pickup and drop off times can be monitored.
- √ **Improved Logistics** - Production machinery has already reached a high level of productivity. Further increases in overall manufacturing efficiency must come from logistics. For example, in many manufacturing facilities, about 75% of each work piece cycle time consists of transportation and waiting. An AGV System can link information about material flow and supply the workstation as demand arises. In general, AGV Systems improve the organization and execution of materials transportation.

- √ **Improved Image / Better Housekeeping** - An AGV System improves plant organization by maintaining clear aisles and organized workstations. Since pickup and drop off stations are fixed and dedicated, operators are able to keep their workstations more organized. This improves the workplace environment for employees and creates a positive image for plant visitors and prospective customers.
- √ **Better Discipline** - An AGV System forces discipline in plant operations. Material flow in and out are scheduled by the AGV System controls. Unnecessary raw, finished or packing materials do not clog aisles and workstations.

2.1.1.3 Possible market applications

AGV systems provide reliable horizontal transportation when space is at a premium and flexibility is critical. For example:

- **Food and Beverage -** High throughput and small traffic areas are common in the food and beverage industry.

  Dual load handling vehicles, such as the one proposed with AGAVE, are best suited to move loads from palletizers directly to the shipping docks or within warehousing operations.
- **Manufacturing -** Moving products to or from work cells in a timely manner is an optimal use for an AGV. A shuttle or fork style vehicle can deliver the load to a static interface point, saving the customer the cost of powering stands in a work cell.
- **Pharmaceutical -** Transportation of raw materials as well as finished product is typical in this industry. Controlled transportation and product identification, as well as safe movement throughout the facility, are key to AGV installations.
- **Automotive -** The automotive industry utilizes AGVs in a number of applications. Many assembly plants now install AGVs as the build deck for their new model cars and trucks. Other sites use AGVs to deliver parts and kits to the assembly line, ensuring that the stations never stop the process.
- **Warehousing** - Movement of finished goods and bulk materials to and from a warehouse is easily accomplished with dual conveyor, lift deck or fork type vehicles. Configurations allow for transportation of 1-4 loads at a time.
- **Roll Handling -** Awkward rolls of paper, plastics or textiles are easily and safely be handled by AGVs . Handling these rolls by the core, “eye to the sky” or on the bilge will drastically reduce the opportunity for product damage.
- **Mail processing -** A simple Automated Guided Vehicle System can provide substantial relief to a complex mail processing operation. In a busy environment like mail handling facilities, Automated Guided Vehicles (AGVs) are successfully used to transport pallets of mail into processing areas.

AGVs have proven to offer increased safety over conventional forklift operators. With critical and daily deadlines to meet, the U.S. mail system benefits from the dependable and constant operation of the AGVs. Reduced product damage, on-time deliveries, and no accidents make AGVs an attractive option.

- **Newspapers upgrades -** The primary purpose of the AGV System is to deliver rolls of newsprint typically to as many as 40 printing press reel stands (10 stands per press). Rolls are retrieved from a receiving storehouse that holds up to 1,000 rolls. The rolls are delivered to a stripper-prep station and then to either a press reel stand or a 27-lane, 265- position buffer zone, lay down area. The AGVs use RF modems to continuously communicate with the Host, thus providing a large degree of flexibility for guidepath tuning.

  In addition to delivering rolls to the presses and laydown, the AGVs also cart away waste paper and spent newsprint roll cores. In addition, changeover rolls (partially used rolls over 35 inches in diameter) and butt rolls (diameters from 6-1/2 inches up to 35 inches) are handled by the AGVs. Damaged or unusable rolls are deposited in a reject area for future disposal.
- **Plastic Manufacturing** – for example, Rehrig Pacific manufactures returnable plastic display and transport crates for many different industries, as well as curbside recycling bins, waste carts, & plastic pallets. Many of Rehrig's products are custom designed for specific client needs. In 2002, Rehrig Pacific installed a standard, laserguided fork-type AGV with a couple of application specific features at their Lawrenceville, GA facility.

  Finished product is manually moved from the mammoth injection molding machines and stacked onto pallets. Stacked pallets are placed onto a conveyor and delivered to stretch-wrapping stations. A central controller routes the AGV to the stack area for delivery of palletized finished product. Once the pallet is on-board, the AGV delivers and transfers the load to the outbound conveyor. The AGV then moves to a holding area for empty pallets, retrieves an empty, and delivers it to the packing area.
- **Nuclear waste handling –** Another important usage could be in the treatment of dangerous materials.

2.1.2 Localization system and algorithms

2.1.2.1 Description of result

Ultra-wideband is an emerging technology with enormous market potential. As it was shown before, it can be used in supply chain management, healthcare and sensor networks. The supply chain management industry has projected market size of US$5 billion in year 2008 rising to

US$20 billion by year 2012. Ultra-wideband (UWB) is a license-free low-power radio transmission scheme with an enormous bandwidth of up to 7.5GHz.

The use of UWB radio will bring significant benefits, such as reduced risk of interfering with sensitive medical equipment in hospital/healthcare applications, very precise positioning for the logistics and retail industries, ability to locate people through smoke and obstacles in hazardous search-and-rescue missions and more.

Despite UWB's low power and short range, the system may be scaled up to serve thousands of nodes over hundreds of meters using networking techniques.

The localization system provided with this project is a mean to accurately determine the position of an object even in NLOS conditions;

For most outdoor applications, systems such as GPS provide users with accurate position estimates. However, reliable range-based localization using radio signals in indoor or urban environments can be a problem due to multipath fading and Line-of-Sight (LOS) blockage.

The measurement bias introduced by these delays causes significant localization error, even when using additional sensors such as an Inertial Measurement Unit (IMU) to perform outlier rejection.

We are developing an algorithm for accurate indoor localization of a sensor in a network of known beacons. The sensor measures the range to the beacons using an Ultra-Wideband (UWB) signal and uses statistical inference to infer and correct for the bias due to LOS blockage in the range measurements. We show that a particle filter can be used to estimate the joint distribution over both pose and beacon biases.

We use the particle filter estimation technique specifically to capture the non-linearity of transitions in the beacon bias as the sensor moves.

2.1.2.2 Possible market applications

The main market applications of this location system could be:

- Tags
- Intrusion Detection Radars
- Precision Geolocation Systems
- Proximity Fuzes
- Precise real time location (for example people in a building, firefighters, doctors in hospitals)

With few minor software adjustments, a UWB system such the one designed for AGAVE project has multifarious scenarios of application, beside the intended indoor positioning one:

- Low Data Rate (LDR) Applications: the use of very short pulses in impulse radio transmission, and careful signal and architecture design, facilitate the design of very simple transmitters, permitting extreme low energy consumption and thus long-life battery-operated devices, which are mainly used in low data rate networks with low duty cycles. Nevertheless, the receiver design remains the major challenge. Energy

detection receivers are a promising approach to build simple receivers. Energy management schemes may alleviate the strict energy bounds imposed by batteries. Surveillance of areas difficult to access by humans can be achieved by the deployment of sensor networks. The inherent noise-like behaviour of UWB systems makes robust security systems highly feasible. They are not only difficult to detect, but also excel in jamming resistance. These characteristics are essential, not only for traditional security alarm systems, but also for Wireless Body Area Networks (WBANs), which are envisaged for medical supervision. Due to the simple transceiver architecture and the thereby expected low costs of transceivers, the number of devices to be employed can be over dimensioned. With this approach, a certain percentage of nodes may fail (due to device failure, bad transmission conditions etc.) without affecting the functioning of the system as such. Deliberately designing devices with higher failure probability will again lower the cost of a single device. For complementing smart homes, actuators can be controlled by a central operator, making human intervention unnecessary. Positioning with previously unattained precision, tracking, and distance measuring techniques, as well as accommodating high node densities due to the large operating bandwidth is also possible. Many routing protocols are known which reduce control-overhead using location information. Today's indoor solutions use either infrared or ultrasonic approaches. The former requires line-of-sight-propagation which can not be guaranteed, and the latter has the disadvantage of propagating with limited penetration. Simple UWB radio technology may fill this gap between demand and physical constraints, and is currently under development. For industrial needs, e.g. in the automotive field, distance measuring systems are yet another example for the deployment of UWB systems as logistics will also profit from highly precise location determination.

- High Data Rate (HDR) Applications: high data rate applications of UWB wireless technology have initially drawn much attention, since many of the applications are suited to the consumer market. Hence, commercial interest in technology development, standards and regulation is very high. The very definition of ultra wideband – a bandwidth exceeding 500 MHz (for carrier frequencies above 2.4 GHz) and an extremely low power spectral density (75nW/MHz between 3.1-10.6GHz, according to FCC rules), makes UWB the perfect candidate technology for these kinds of scenarios. The problem of designing transceivers with reasonable complexity, also suitable for handheld devices, is one of the main challenges for high-rate applications. Robustness against jamming is also very important, as a large number of electrical devices emitting narrowband noise are usually found in home and office environments, as well as interfering signals from other wireless services operating in sections of the UWB bandwidth.

Main application areas include:

- Internet Access and Multimedia Services: Regardless of the envisioned environment (home, office, hot spot), very high data rates (> 1 Gbit/s) have to be provided – either due to high peak data rates, high numbers of users, or both.
- Wireless peripheral interfaces: A growing number of devices (laptop, mobile phone, PDA, headset, etc.) are employed by users to organize themselves in their daily life. The required data exchange is expected to happen as conveniently as possible or even automatically. Standardized wireless interconnection is highly desirable to replace cables and proprietary plugs. It has to be emphasized, however, that wireless solutions in this context will be attractive mainly for battery-powered devices without the need for an external power supply.
- Location based services: To supply the user with the information he/she currently needs, at any place and any time (e.g. location aware services in museums or at exhibitions), the users' position has to be accurately measured. UWB techniques may be used to accommodate positioning techniques and data transmission in a single system for indoor and outdoor operation.
- Home Networking and Home Electronics: one of the most promising commercial application areas for UWB technology is wireless connectivity of different home electronic systems. It is thought that many electronics manufacturers are investigating UWB as the wireless means to connect together devices such as televisions, DVD players, camcorders, and audio systems, which would remove some of the wiring clutter in the living room. This is particularly important when we consider the bit rate needed for high-definition television that is in excess of 30Mbps over a distance of at least a few meters.

– Wireless Body Area Networks (WBAN): WBANs are another example of how our life could be influenced by UWB. Probably the most promising application in this context is medical body area networks. Due to the proposed energy efficient operation of UWB, battery driven handheld equipment is feasible, making it perfectly suitable for medical supervision. Moreover, UWB signals are inherently robust against jamming, offering a high degree of reliability, which will be necessary to provide accurate patient health information and reliable transmission of data in a highly obstructed radio environment. The possibility to process and transmit a large amount of data and transfer vital information using UWB wireless body area networks would enable tele-medicine to be the solution for future medical treatment of certain conditions. In addition, the ability to have controlled power levels would provide flawless connectivity between body-distributed networks. UWB also offers good penetrating properties that could be applied to imaging in medical applications; with the UWB body sensors this application could be easily reconfigured to adapt to the specific tasks and would enable high data rate connectivity to external processing networks (e.g. servers and large workstations).